

Sparse Spectrahedral Shadows for State Estimation and Reachability Analysis: Set Operations, Validations and Order Reductions

Chengrui Wang, Haohao Qiu, Sibao Yao and James Lam*, *Fellow, IEEE*

Abstract—Set representations are the foundation of various set-based approaches in state estimation, reachability analysis and fault diagnosis. In this paper, we investigate *spectrahedral shadows*, a class of nonlinear geometric objects previously studied in semidefinite programming and real algebraic geometry. We demonstrate spectrahedral shadows generalize traditional and emerging set representations like ellipsoids, zonotopes, constrained zonotopes and ellipsotopes. Analytical forms of set operations are provided including linear map, linear inverse map, Minkowski sum, intersection, Cartesian product, Minkowski-Firey L_p sum, convex hull, conic hull and polytopic map, all of which are implemented without approximation in polynomial time. In addition, we develop set validation and order reduction techniques for spectrahedral shadows, thereby establishing spectrahedral shadows as a set representation applicable to a range of set-based tasks.

Index Terms—Set Representation, Spectrahedral Shadow, Reachability analysis, State estimation, Fault detection

I. INTRODUCTION

Set-based approaches have been widely used in fields such as state estimation (SE) [1], [2], reachability analysis (RA) [3], [4] and fault diagnosis (FD) [5], [6], since many of them require handling worst-case uncertainties (e.g., measurement noise, modeling error, and process disturbance) and establishing reliable boundaries for system behaviors. As the common foundation of these fields, set representations directly determine the accuracy, the efficiency and the space overhead for implementing set-based approaches.

A. Existing Convex Set Representations

The topic of this paper is convex set representations. In SE, RA and FD, traditional set representations include polyhedrons, ellipsoids, zonotopes and support functions [7], [8], and common set operations involve affine map, Minkowski sum, intersection, convex hull and affine inverse map [6], [9]. Polyhedrons have vertex representation (V-polytopes) and hyperplane representation (H-polyhedrons). The former is closed under affine map, Minkowski sum and convex hull, and the

latter is closed under affine inverse map and intersection. However, the complexity of conversion between V-polytopes and H-polyhedrons is NP-hard [10], which makes approaches using polyhedrons extremely time-consuming when dimension exceeds about 5. To the contrary, working with ellipsoids is highly efficient [6]. Ellipsoids can represent practical quadratic boundaries without approximation, such as the bounded energy constraints and the confidence region of Gaussian distribution. Unfortunately, ellipsoids are not closed under Minkowski sum, convex hull and intersection, and hence need additional ellipsoidal approximation after these operations, resulting in loss of accuracy. In comparison, zonotopes are a high efficient set-representation closed under affine map and Minkowski sum, but zonotopes cannot exactly represent non-centrosymmetric or nonlinear boundaries. Support functions can characterize all non-empty closed convex sets, and have analytical expressions for affine map and Minkowski sum [3]. But in practice, support functions need approximation to implement intersection [11] and cannot check emptiness, which restricts the application of support functions on tasks such as set-membership estimation [9] and collision avoidance [12].

Recently, constrained zonotopes [6], [13], ellipsotopes [12] and constrained convex generators (CCGs) [14], [15] have been developed to overcome the shortcoming of traditional set representations. Besides the inherent advantages of zonotopes, constrained zonotopes can represent arbitrary convex bounded polytopes [6, Theorem 1], and are closed under intersection and convex hull [13, Theorem 5]. To handle mixed polytopic and ellipsoidal uncertainties, ellipsotopes are proposed based on constrained zonotopes through introducing an indexed set and the Cartesian product of p -norm balls. Ellipsotopes unify constrained zonotopes and ellipsoids, and inherit the closure properties under all set operations of constrained zonotopes, except for convex hull [12, Proposition 8]. Following ellipsotopes, CCGs further relax the Cartesian product of p -norm balls as the Cartesian product of arbitrary constraints, such that convex hull can be implemented without approximation under an implication assumption.

B. Overview

This paper investigates *spectrahedral shadows*, a class of nonlinear convex geometry previously studied by semidefinite programming [16], [17] and real algebraic geometry [18], [19]. Different from the previous research, we focus on necessary

*Corresponding author: James Lam (Email:james.lam@hku.hk).

Chengrui Wang, Haohao Qiu and James Lam are with the Department of Mechanical Engineering, The University of Hong Kong, Pokfulam, Hong Kong. Sibao Yao is with the College of Intelligent Systems Science and Engineering, Harbin Engineering University, Harbin 150001, China

techniques to apply spectrahedral shadows on SE, RA and FD. Specifically, our work includes

- 1) Section III-A provides the nonconservative realization of set operations including linear map, linear inverse map, Minkowski sum, intersection, Cartesian product, Minkowski-Firey L_p sum, convex hull, conic hull and polytopic map. We show that all of them can be implemented within polynomial time.
- 2) Section III-B is the implementation of common set validations in SE, RA and FD, including point containment, emptiness check and boundedness check.
- 3) Section III-C gives the nonconservative methods to convert H-polyhedrons, ellipsoids, zonotopes, constrained zonotopes and ellipsotopes to spectrahedral shadows.
- 4) Section IV discusses the strategies to reduce the complexity of high order spectrahedral shadows. Acceleration strategy is also provided utilizing the sparsity possessed by spectrahedral shadows in practice.

Through the above work, spectrahedral shadows are established as a set representation applicable to set-based SE, RA and FD. Compared with the advanced set representations like ellipsotopes [12] and CCGs [15], [20], spectrahedral shadows are with the following characteristics

- 1) (More compact representation) Spectrahedral shadows is concisely represented by one linear matrix inequality (LMI), instead of the form of ellipsotopes and CCGs that requires the center, generators, linear equalities, p -norm balls, index set and even more complex constraints. Such conciseness makes spectrahedral shadows representing high order sets more compactly and efficiently. Our numerical results show that the space overhead of high-order spectrahedral shadows is reduced by about 55%-85% compared with the same set represented by ellipsotopes and CCGs. For high order sets, reducing space overhead means improving the efficiency. Because time consumption of set operations is positively correlated with the input scale of set representations, and using order reduction techniques to reduce space overhead also results in extra time consumption.
- 2) (More supported set operations) Besides the exact set operations realized by ellipsotopes [12] and CCGs [14], spectrahedral shadows additionally support affine inverse map, Minkowski-Firey L_p sum, conic hull and polytopic map. Affine inverse map is useful for tasks such as computing the unguaranteed detectable faults set [21], backward reachability analysis [22], [23] and the set membership estimation with limited sensors (see Section V for example). Thorough Minkowski-Firey L_p , exact reachable sets can be attained for the task in [3]. With polytopic map, spectrahedral shadows are able to achieve exact SE and RA on uncertain linear parameter-varying (LPV) systems [5], [20]. Moreover, the exact convex hull can be directly obtained for bounded spectrahedral shadows, instead of requiring additional assumptions like CCGs (see [14, Theorem 1]) or outer approximation like ellipsotopes (see [12, Proposition 8]).

II. PRELIMINARIES

A. Notations

The $n \times m$ null matrix and the $n \times m$ matrix full of 1 are denoted as $\mathbf{0}^{n \times m}$ and $\mathbf{1}^{n \times m}$, and the subscript will be omitted for brevity (e.g., $\mathbf{0}$) when there is no ambiguity. The n -dimensional identity matrix is denoted as I_n . The notation \mathbb{N} represents the natural numbers. The symbols \mathbb{R}^n and \mathbb{S}^n denote the n -dimensional vector space and the symmetric matrix space over real numbers. For $x, y \in \mathbb{R}^n$, x_i denotes the i -th component of x , and $x \geq y$ means $x_i \geq y_i, \forall 1 \leq i \leq n$ (and similar goes for $x \leq y, x > y$ and $x < y$). For $X \in \mathbb{R}^{n \times m_1}$ and $Y \in \mathbb{R}^{n \times m_2}$, $[X \ Y]$ denotes the matrix concatenation of X and Y , $X_{[i,j]}$ denotes the element in the i -th row and j -th column of X , and $X_{[i,*]}$ and $X_{[*],j}$ are the i -th row and the j -th column of X , respectively.

For $X \in \mathbb{R}^{n \times n}$, $\text{dvec}(X)$ denotes a vector such that $\text{dvec}(X)_i = X_{[i,i]}, \forall 1 \leq i \leq n$. For $X, Y \in \mathbb{S}^n$, $X \succeq Y$ means $X - Y$ is a positive semidefinite matrix (and similar rules apply for $X \preceq Y, X \succ Y$ and $X \prec Y$), and the vector $\text{tvec}(X) \in \mathbb{R}^{n(n+1)/2}$ is obtained by vectorizing the upper (or lower) triangular part of X by column. For $X_1 \in \mathbb{R}^{n_1 \times m_1}, X_2 \in \mathbb{R}^{n_2 \times m_2}, \dots, X_v \in \mathbb{R}^{n_v \times m_v}$, we define

$$\text{diag}(X_1, X_2, \dots, X_v) = \begin{bmatrix} X_1 & \mathbf{0} & \cdots & \mathbf{0} \\ \mathbf{0} & X_2 & \cdots & \mathbf{0} \\ \vdots & \vdots & \ddots & \vdots \\ \mathbf{0} & \mathbf{0} & \cdots & X_v \end{bmatrix}.$$

For $X_1, X_2, \dots, X_v \in \mathbb{R}^{n \times m}$, the convex combination of X_1, X_2, \dots, X_v is a matrix set defined as $\text{conv}\{T_1, T_2, \dots, T_v\} = \{\sum_{i=1}^v \theta_i T_i : \sum_{i=1}^v \theta_i = 1, \theta_i \geq 0, 1 \leq i \leq v\}$.

Consider two sets $X, Y \subset \mathbb{R}^n$. The notation \overline{X} , $\text{bd}(X)$, $|X|$ and $\mathbb{P}(X)$ denote the closure, the boundary, the cardinality and the power set of X , respectively. The notation $\text{dim}(X)$ denotes the dimension of the affine hull of X . The image and preimage of X under the map f are represented by $f \circ X$ and $X \circ f$, respectively. The convex hull of X and Y is defined as $\text{conv}(X \cup Y) = \{\theta_1 x + \theta_2 y : x \in X, y \in Y, \theta_1, \theta_2 \geq 0, \theta_1 + \theta_2 = 1\}$. The Minkowski sum, Cartesian product and difference of X and Y are denoted by $X \oplus Y = \{x + y : x \in X, y \in Y\}$, $X \times Y = \{(x, y)^T : x \in X, y \in Y\}$ and $X \setminus Y = \{x : x \in X, x \notin Y\}$, respectively. The unit p -norm ball in \mathbb{R}^n is denoted by $\mathcal{B}_p^n = \{x \in \mathbb{R}^n : \|x\|_p \leq 1\}$. The volume of X is denoted as $\text{vol}(X)$, and the volume ratio of X and Y is defined as $\Delta V = (\frac{\text{vol}(X)}{\text{vol}(Y)})^{\frac{1}{n}}$.

B. Set Representations

This section introduces traditional and emerging convex set representations [6], [12], [24], [25] used in SE, RA and FD.

1) *H-polyhedron*: *H-polyhedrons* are a collection of sets represented by the intersection of finite half-spaces, i.e., $\mathcal{P}(A, b) = \{x \in \mathbb{R}^n : Ax \leq b\}$, where $A \in \mathbb{R}^{n_c \times n}$ and $b \in \mathbb{R}^{n_c}$ define the hyperplanes.

2) *Ellipsoid*: *Ellipsoids* are a collection of sets represented by $\mathcal{E}(c, Q) = \{x \in \mathbb{R}^n : (x - c)^T Q^{-1} (x - c) \leq 1, Q \succ 0\}$, where $Q \in \mathbb{S}^n$ and $c \in \mathbb{R}^n$ is called the *center*.

3) **Zonotope**: Zonotopes are a collection of centrosymmetric polytope represented by $\mathcal{Z}(c, G) = \{x \in \mathbb{R}^n : x = c + G\xi, \|\xi\|_\infty \leq 1\}$, where $c \in \mathbb{R}^n$ and $G \in \mathbb{R}^{n \times n_g}$ are called the *center* and *generator matrix*.

4) **Constrained Zonotope**: Constrained zonotopes are a collection of polytopes in zonotopic form. A constrained zonotope is represented by $\mathcal{CZ}(c, G, A, b) = \{x \in \mathbb{R}^n : x = c + G\xi, \|\xi\|_\infty \leq 1, Ax = b\}$, where $A \in \mathbb{R}^{n_c \times n_g}$ and $b \in \mathbb{R}^{n_c}$ together define the constraints, and $c \in \mathbb{R}^n$ and $G \in \mathbb{R}^{n \times n_g}$ are consistent with zonotopes.

5) **Ellipsotope**: Ellipsotopes are the unification of ellipsoids and constrained zonotopes. An ellipsotope is represented by $\mathcal{E}_p(c, G, A, b, \mathcal{J}) = \{x \in \mathbb{R}^n : x = c + G\xi, \|\xi(J)\|_p \leq 1, \forall J \in \mathcal{J}, Ax = b\}$, where $p \geq 1$, $\mathcal{J} = \{J_1, J_2, \dots, J_{|\mathcal{J}|}\} \subset \mathbb{P}(\mathbb{N})$ is called a *indexed set*, each $\xi(J)$ is a part of the vector ξ indexed by \mathcal{J} , and $c \in \mathbb{R}^n$, $G \in \mathbb{R}^{n \times n_g}$, $A \in \mathbb{R}^{n_c \times n_g}$ and $b \in \mathbb{R}^{n_c}$ are consistent with constrained zonotopes.

C. Computational Complexities Analysis

For the convenience of subsequent analysis, we introduce some conventions and known results about computational complexities used in this paper. We use big O notation (i.e., $\mathcal{O}(\cdot)$) to analyze the worst-case of asymptotic complexities and use ω to denote the exponent of matrix multiplication. Currently, the bound of ω is $\omega \leq 2.372$ [26].

Consistent with [12] and [27], we consider the time complexity of all matrix operations except for matrix initialization and matrix concatenation. Specifically, if we consider the complexity of arithmetic for each element as $\mathcal{O}(1)$, then we can conclude the following complexity of matrix operations:

- 1) For $X, Y \in \mathbb{R}^{m \times n}$, $X + Y$ is $\mathcal{O}(mn)$.
- 2) For $X \in \mathbb{R}^{m \times n}$, $Y \in \mathbb{R}^{n \times l}$, XY is $\mathcal{O}(mnl)$.
- 3) For $X \in \mathbb{R}^{n \times n}$, X^{-1} is $\mathcal{O}(n^\omega)$.
- 4) For $X \in \mathbb{R}^{m \times n}$, the singular value decomposition (SVD) is $\mathcal{O}(\tilde{m}\tilde{n})$, where $\tilde{m} = \max\{m, n\}$ and $\tilde{n} = \min\{m, n\}$.

Moreover, consider the following dual form of semidefinite programming (SDP) problem:

$$\min_x b^T x \quad \text{s.t.}, \quad A + \sum_{i=1}^n x_i A_i \succeq 0, \quad (1)$$

where $b, x \in \mathbb{R}^n$ and $A, A_1, \dots, A_n \in \mathbb{S}^s$. For numerically solving the SDP problem (1) using interior point method with given accuracy, the state-of-the-art algorithm runs in $\mathcal{O}(\sqrt{s}(ns^2 + n^\omega + s^\omega))$ time [28, Theorem I.2].

III. SPECTRAHEDRAL SHADOWS

We first introduce the definition of *spectrahedral shadows*.

Definition 1: A set $\mathcal{S} \subset \mathbb{R}^n$ is a *spectrahedral shadow* if there exist $A, A_1, A_2, \dots, A_n, B_1, B_2, \dots, B_m \in \mathbb{S}^s$ such that

$$\mathcal{S} = \{x \in \mathbb{R}^n : \exists y \in \mathbb{R}^m, A + \sum_{i=1}^n x_i A_i + \sum_{i=1}^m y_i B_i \succeq 0\}, \quad (2)$$

where s and m are the *size* and *lifted dimension* of spectrahedral shadows, respectively. For brevity, a spectrahedral shadow in the form of (2) is abbreviated as $\langle A, \{A_i\}_{i=1}^n, \{B_i\}_{i=1}^m \rangle$.

Spectrahedral shadows have also been called *SDP representable sets* [29] or *projections of spectrahedrons* [17] for the research of semidefinite representability. Moreover, spectrahedral shadows with zero lifted dimension, i.e., $\langle A, \{A_i\}_{i=1}^n \rangle$, are called *spectrahedrons*.

Remark 1: When applied to SE, RA and FD, spectrahedral shadows have sparse structures (see Section IV-C). To store $\langle A, \{A_i\}_{i=1}^n, \{B_i\}_{i=1}^m \rangle$ in practice, we only need to store n, s, m and an $s \times s(1 + n + m)$ sparse matrix by stacking the upper triangular part of $A, \{A_i\}_{i=1}^n$ and $\{B_i\}_{i=1}^m$ by column.

Lemma 1 introduces some known conclusions used in this paper.

Lemma 1 ([16]): There are the following properties about spectrahedral shadows:

- 1) A spectrahedral shadow is not necessarily a bounded set.
- 2) A spectrahedral shadow is not necessarily a closed set.
- 3) Consider a set $X = \{x \in \mathbb{R}^n : f_i(x) \leq 0, i = 1, 2, \dots, m\}$, where each $f_i(x)$ is a polynomial and X has the nonempty interior. If each $f_i(x)$ is quasi-convex on X , X can be represented as a spectrahedral shadow.

Example 1: We give a few examples to illustrate Lemma 1. For the point 1), the spectrahedral shadow $\langle A, \{A_i\}_{i=1}^2 \rangle$ with $A = I_2$, $A_1 = 1.2 \times (\mathbf{1} - I_2)$ and $A_2 = \text{diag}(1, 0)$ is the region restricted by the parabola $\{x \in \mathbb{R}^2 : 1 - 1.44x_1^2 + x_2 = 0\}$ (see Fig. 1(a)), and hence is an unbounded set. For the point 2), the spectrahedral shadow $\langle A, \{A_i\}_{i=1}^1, \{B_i\}_{i=1}^1 \rangle$ with $A = \mathbf{1} - I_2$, $A_1 = \text{diag}(1, 0)$ and $B_1 = \text{diag}(0, 1)$ is the open interval $(0, \infty)$. For the point 3), all polynomials in the set $\{x \in \mathbb{R}^3 : -x_1 \leq 1, x_1^2 + x_2^2 + x_3^2 - x_1x_2 + x_1x_3 - 2x_2x_3 - x_1 + 3x_2 - 3x_3 \leq -2, x_1^2 + 2x_2^2 + 2x_1x_2 + 2x_1x_3 + 2x_2x_3 - 2x_1 - 2x_2 \leq 0, x_1^2 + x_2^2 + x_1x_2 - x_1x_3 + 3x_1 + x_2 - x_3 \leq -2, 3x_1^3 - 2x_2^3 + x_3^3 + 4x_1^2x_2 + 8x_1^2x_3 - 4x_1x_2^2 + 4x_1x_3^2 + x_2x_3^2 + 8x_1x_2x_3 - 5x_1^2 - 2x_2^2 - x_3^2 - 8x_1x_2 + 2x_2x_3 - 4x_1 - 4x_2 \leq 0\}$ are convex (a special case of quasi-convex) on this set. This set can be characterized by a spectrahedron concisely, i.e., $\langle A, \{A_i\}_{i=1}^2 \rangle$ with

$$A = \begin{bmatrix} 1 & -1 & 1 \\ * & -1 & 1 \\ * & * & -1 \end{bmatrix}, A_1 = \begin{bmatrix} 1 & 1 & 1 \\ * & 0 & -1 \\ * & * & 0 \end{bmatrix},$$

$$A_2 = \begin{bmatrix} 0 & -1 & 1 \\ * & -1 & -1 \\ * & * & 1 \end{bmatrix}, A_3 = \begin{bmatrix} 0 & 1 & 0 \\ * & 1 & -1 \\ * & * & 1 \end{bmatrix},$$

where the figure is shown in Fig. 1(b).

Section III-C provides methods to convert existing common set representations into spectrahedral shadows. For converting the sets represented by convex polynomial inequalities to spectrahedral shadows, there is an available construction techniques known as the moment method, where the details can be found in [30], [31].

A. Set Operations

Spectrahedral shadows are known to be closed under operations including affine map, Minkowski sum, intersection, Cartesian product and convex hull [17], [18], [32]. However, except for the intersection and convex hull, general expressions

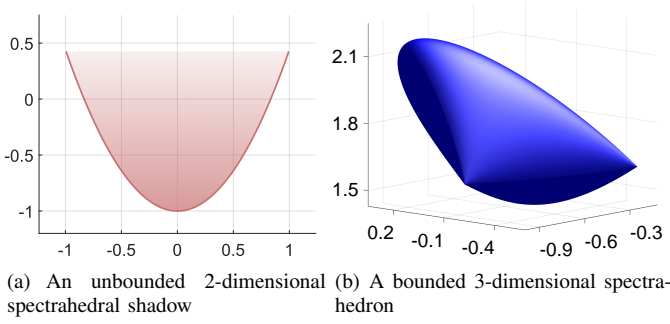


Fig. 1. Spectrahedral shadows given in Example 1.

have not been systematically seen in the literature¹. Moreover, in fields such as set-based SE, RA and FD, our concern is how to perform these set operations in a unified and iterable manner, and more importantly, whether such operations can be performed in a reasonable time (e.g., polynomial time). These issues are what we aim at addressing in this section.

1) Affine Map: Since an affine map comprises a translation and a linear map, we first give the expression of translation and then give that of linear map for spectrahedral shadows.

Lemma 2 (Translation): For any $b \in \mathbb{R}^n$ and nonempty $\mathcal{S} = \langle \Lambda, \{A_i\}_{i=1}^n, \{B_i\}_{i=1}^m \rangle$ with size s , we have

$$\mathcal{S} + b = \langle \Lambda - \sum_{i=1}^n b_i A_i, \{A_i\}_{i=1}^n, \{B_i\}_{i=1}^m \rangle. \quad (3)$$

The computational complexity is $\mathcal{O}(ns^2)$.

Proof: For arbitrary $x \in \mathcal{S}$ and $z = x + b$, we have $z - b \in \mathcal{S}$. It follows from Definition 2 that $\exists y \in \mathbb{R}^m, \Lambda + \sum_{i=1}^n (z_i - b_i) A_i + \sum_{i=1}^m y_i B_i \succeq 0$, thereby leading to (3).

Complexity: Computing $\Lambda - \sum_{i=1}^n b_i A_i$ needs $\mathcal{O}(ns^2)$ multiplications and $\mathcal{O}(ns^2)$ matrix subtractions. By omitting the constant coefficients, the overall complexity is $\mathcal{O}(ns^2)$. ■

Then we introduce Lemma 3 as the foundation to establish the general expression of linear map.

Lemma 3 (Invertible linear map): For any invertible matrix $T \in \mathbb{R}^{n \times n}$ and nonempty $\mathcal{S} = \langle \Lambda, \{A_i\}_{i=1}^n, \{B_i\}_{i=1}^m \rangle$ with size s , we have

$$T \circ \mathcal{S} = \langle \Lambda, \{ \sum_{i=1}^n T_{[i,j]}^{-1} A_i \}_{j=1}^n, \{B_i\}_{i=1}^m \rangle. \quad (4)$$

The computational complexity is $\mathcal{O}(n^\omega + n^2 s^2)$.

Proof: For any $x \in \mathcal{S}$ and $z = Tx$, we have $T^{-1}z \in \mathcal{S}$ as T is invertible, which is equivalent to $\exists y \in \mathbb{R}^m, \Lambda + \sum_{i=1}^n x_i T_{[i,j]}^{-1} A_i + \sum_{i=1}^m y_i B_i \succeq 0$, thereby leading to (4).

Complexity: The complexity to obtain T^{-1} is $\mathcal{O}(n^\omega)$, where the constant ω has been defined in Section II-C. Computing $\sum_{i=1}^n T_{[i,j]}^{-1} A_i$ for all $1 \leq j \leq n$ requires $\mathcal{O}(n^2 s^2)$ multiplications and $\mathcal{O}(n(n-1)s^2)$ matrix additions. Thus, the overall complexity is $\mathcal{O}(n^\omega + n^2 s^2)$. ■

¹[32, Section 4.1.1] asserted that the mentioned set operations are fully algorithmic, but no expressions are given except for the intersection (see Lemma 4) and a special case of conic hull (see Remark 5).

Proposition 1 (Linear map): For arbitrary $T \in \mathbb{R}^{l \times n}$ and nonempty $\mathcal{S} = \langle \Lambda, \{A_i\}_{i=1}^n, \{B_i\}_{i=1}^m \rangle$ with size s , we have

$$T \circ \mathcal{S} = \langle \Lambda^t, \{ \sum_{i=1}^n U_{[i,j]}^T A_i^t \}_{j=1}^l, \{B_i^t\}_{i=1}^{m_t} \rangle \quad (5)$$

with

$$\Lambda^t = \text{diag}(\Lambda, \mathbf{0}),$$

$$A_i^t = \begin{cases} \text{diag}(\sum_{j=1}^n D_{[i,i]}^{-1} V_{[i,j]}^T A_j, \mathbf{0}), & 1 \leq i \leq r_t \\ \text{diag}(\mathbf{0}, \Gamma^{i-r_t}), & r_t + 1 \leq i \leq l \end{cases},$$

$$B_i^t = \begin{cases} \text{diag}(B_i, \mathbf{0}), & 1 \leq i \leq m \\ \text{diag}(\sum_{j=1}^n V_{[i-m+r_t,j]}^T A_j, \mathbf{0}), & m+1 \leq i \leq m_t \end{cases},$$

$$\Gamma_{[j,k]}^i = \begin{cases} 1, & j = k = i \\ -1, & j = k = l - r_t + i \quad 1 \leq i \leq l - r_t, \\ 0, & \text{otherwise} \end{cases}$$

where $\Lambda^t, A_i^t, B_i^t \in \mathbb{S}^{s+2(l-r_t)}$, $\Gamma^i \in \mathbb{S}^{2(l-r_t)}$, $m_t = m + n - r_t$, $r_t = \text{rank}(T)$, and $T = UDV^T$ is the SVD such that $D_{[i,i]}$ is the i -th largest singular value of T . The computational complexity is $\mathcal{O}(\tilde{l}^4 + \tilde{l}^3 s + \tilde{l}^2 s^2)$, where $\tilde{l} = \max\{l, n\}$.

Proof: Let $\mathcal{S}_t^1 = V^T \circ \mathcal{S}$ and $\mathcal{S}_t^2 = D \circ \mathcal{S}_t^1$. Then we have $T \circ \mathcal{S} = U \circ \mathcal{S}_t^2$. Since V^T is an orthogonal matrix, it yields $\mathcal{S}_t^1 = \langle \Lambda, \{ \sum_{i=1}^n V_{[i,j]}^T A_i \}_{i=1}^n, \{B_i\}_{i=1}^m \rangle$ by Lemma 3. To formulate $\mathcal{S}_t^2 = D \circ \mathcal{S}_t^1$, assume that $z = Dx$ and $x \in \mathcal{S}_t^1$. According to Definition 2, $x \in \mathcal{S}_t^1$ is equivalent to

$$\exists y \in \mathbb{R}^m, \Lambda + \sum_{i=1}^n x_i \sum_{j=1}^n V_{[i,j]}^T A_j + \sum_{i=1}^m y_i B_i \succeq 0. \quad (6)$$

Since D is a diagonal matrix, $z = Dx$ can be rewritten as

$$z_i = \begin{cases} D_{[i,i]} x_i, & 1 \leq i \leq r_t \\ 0, & r_t + 1 \leq i \leq l \end{cases}. \quad (7)$$

Note that $D_{[i,i]} > 0, \forall 1 \leq i \leq r_t$. Substituting (7) into (6), $z = Dx$ and $x \in \mathcal{S}_t^1$ iff $\sum_{i=r_t+1}^l z_i \Gamma^{i-r_t} \succeq 0$ and

$$\exists y \in \mathbb{R}^m, \Lambda + \sum_{i=1}^{r_t} z_i \sum_{j=1}^n D_{[i,i]}^{-1} V_{[i,j]}^T A_j + \sum_{i=1}^m y_i B_i \succeq 0,$$

which yields $\mathcal{S}_t^2 = D \circ \mathcal{S}_t^1 = \{Dx : x \in \mathcal{S}_t^1\} = \langle \Lambda^t, \{A_i^t\}_{i=1}^l, \{B_i^t\}_{i=1}^{m_t} \rangle$. According to Lemma 3, we obtain (5) from $T \circ \mathcal{S} = U \circ \mathcal{S}_t^2$ and $\mathcal{S}_t^2 = \langle \Lambda^t, \{A_i^t\}_{i=1}^l, \{B_i^t\}_{i=1}^{m_t} \rangle$.

Complexity: Conducting SVD for T has $\mathcal{O}(\tilde{l}^2 \tilde{n})$ complexity, where $\tilde{n} = \min\{l, n\}$. The construction of A_i^t for all $1 \leq i \leq l$ requires $\mathcal{O}(r_t(ns^2 + 1))$ multiplications and $\mathcal{O}((n-1)s^2)$ matrix additions, and hence has $\mathcal{O}(r_t ns^2)$ complexity. Similarly, constructing B_i^t for all $1 \leq i \leq l$ has $\mathcal{O}((n-r_t)ns^2)$ complexity. According to Lemma 3, computing (5) based on Λ_t, A_i^t and B_i^t has $\mathcal{O}(l^2(s + 2(l-r_t))^2)$. Since the complexity of all other operations is a lower-order term, the overall complexity is $\mathcal{O}(\tilde{l}^2 \tilde{n} + n^2 s^2 + l^2(s + 2(l-r_t))^2)$, which is further approximated as $\mathcal{O}(\tilde{l}^4 + \tilde{l}^3 s + \tilde{l}^2 s^2)$ using $\tilde{l} = \max\{l, n\}$, $\tilde{n} \leq \tilde{l}$ and $l - r_t \leq \tilde{l}$. ■

2) Affine inverse map: The affine inverse map is useful for set-membership estimation [9] and backward reachability analysis [22], [23]. We provide the expression of the linear inverse map in Proposition 2, which leads to the affine inverse map together with Lemma 2.

Proposition 2 (Linear inverse map): For arbitrary $T \in \mathbb{R}^{n \times l}$ and nonempty $\mathcal{S} = \langle A, \{A_i\}_{i=1}^n, \{B_i\}_{i=1}^m \rangle$ with size s , we have

$$\mathcal{S} \circ T = \langle A, \left\{ \sum_{j=1}^n T_{[i,j]} A_j \right\}_{i=1}^l, \{B_i\}_{i=1}^m \rangle \quad (8)$$

The computational complexity is $\mathcal{O}(l n s^2)$.

Proof: For $x = Tz$, we have $x_i = \sum_{j=1}^l T_{[i,j]} z_j, \forall 1 \leq i \leq n$. Thus, $x \in \mathcal{S}, x = Tz$ iff $\exists y \in \mathbb{R}^m, \Lambda + \sum_{i=1}^n \sum_{j=1}^l T_{[i,j]} z_j A_i + \sum_{i=1}^m y_i B_i \succeq 0$, which yields (8).

Complexity: Computing $\sum_{i=1}^n T_{[i,j]} A_i$ for all $1 \leq j \leq l$ requires $\mathcal{O}(l n s^2)$ multiplications and $\mathcal{O}(l(n-1)s^2)$ matrix additions. The overall complexity is $\mathcal{O}(l n s^2)$. ■

Moreover, Proposition 3 indicates that a set representation cannot be closed under linear inverse map unless this set representation can characterize unbounded sets.

Proposition 3: For a set representation \mathcal{R} , there exists an unbounded set $X \in \mathcal{R}$ if \mathcal{R} is closed under linear inverse maps.

Proof: Without loss of generality, let the singleton set $\{0\} \subset \mathbb{R}^m$ be represented by \mathcal{R} . Consider a linear map $T: \mathbb{R}^n \rightarrow \mathbb{R}^m$ that admits a nontrivial null space $\text{Null}(T)$. By definition, the preimage of $\{0\}$ under T is $\text{Null}(T)$. Since \mathcal{R} is closed under linear inverse maps, we have $\text{Null}(T) \in \mathcal{R}$. ■

Corollary 1: Ellipsoids, zonotopes, constrained zonotopes, V-polytopes and ellipsotopes are not closed under linear inverse maps.

Proof: Corollary 1 directly follows from Proposition 3 since all set representations mentioned above can only represent bounded sets. ■

Remark 2: It should be noted that Corollary 1 only asserts that the mentioned set representations are not closed under general linear inverse maps, but these set representations can be closed with extra assumptions (e.g., the linear inverse map T is invertible [23, Section 4.4.11]).

3) Minkowski sum: Then Proposition 4 shows how to compute the Minkowski sum of spectrahedral shadows.

Proposition 4 (Minkowski sum): Given $\mathcal{S}_1 = \langle A, \{A_i\}_{i=1}^n, \{B_i\}_{i=1}^{m_1} \rangle$ with size s_1 and $\mathcal{S}_2 = \langle \Gamma, \{C_i\}_{i=1}^{n_2}, \{D_i\}_{i=1}^{m_2} \rangle$ with size s_2 , we have

$$\mathcal{S}_1 \oplus \mathcal{S}_2 = \langle \tilde{A}, \{\tilde{A}_i\}_{i=1}^{\tilde{n}}, \{\tilde{B}_i\}_{i=1}^{\tilde{m}} \rangle, \quad (9)$$

where $\tilde{m} = n + m_1 + m_2, \tilde{A}, \tilde{A}_i, \tilde{B}_i \in \mathbb{S}^{s_1+s_2}, \tilde{A} = \text{diag}(\Lambda, \Gamma), \tilde{A}_i = \text{diag}(\mathbf{0}, A_i)$ and

$$\tilde{B}^i = \begin{cases} \text{diag}(-A_i, C_i), & 1 \leq i \leq n \\ \text{diag}(B_{i-n}, \mathbf{0}), & n+1 \leq i \leq n+m_1 \\ \text{diag}(\mathbf{0}, D_{i-n-m_1}), & n+m_1+1 \leq i \leq \tilde{m} \end{cases}.$$

The computational complexity is $\mathcal{O}(n s_1^2)$.

Proof: It is observed that $z = x + u, x \in \mathcal{S}_1, u \in \mathcal{S}_2$ iff $\exists y \in \mathbb{R}^{m_1}, \Lambda + \sum_{i=1}^n (z_i - u_i) A_i + \sum_{i=1}^{m_1} y_i B_i \succeq 0$ and $\exists v \in \mathbb{R}^{m_2}, \Gamma + \sum_{i=1}^{n_2} u_i C_i + \sum_{i=1}^{m_2} v_i D_i \succeq 0$. Let $e = [u, y, v]^T$. The above is further equivalent to $\exists e \in \mathbb{R}^{\tilde{m}}, \tilde{A} + \sum_{i=1}^{\tilde{n}} z_i \tilde{A}_i + \sum_{i=1}^{\tilde{m}} e_i \tilde{B}_i \succeq 0$ and hence yields (9).

Complexity: The complexity to compute $-A^i$ for all $1 \leq i \leq n$ is $\mathcal{O}(n s_1^2)$. The remaining operation is matrix concatenation and hence the overall complexity is $\mathcal{O}(n s_1^2)$. ■

4) Intersection: In the literature, [32] has given the expression of intersection for spectrahedral shadows. Here we introduce this method as the following Lemma 4.

Lemma 4 (Intersection, [32, p. 428]): Given $\mathcal{S}_1 = \langle A, \{A_i\}_{i=1}^n, \{B_i\}_{i=1}^{m_1} \rangle$ with size s_1 and $\mathcal{S}_2 = \langle \Gamma, \{C_i\}_{i=1}^{n_2}, \{D_i\}_{i=1}^{m_2} \rangle$ with size s_2 , we have

$$\mathcal{S}_1 \cap \mathcal{S}_2 = \langle \tilde{A}, \{\tilde{A}_i\}_{i=1}^{\tilde{n}}, \{\tilde{B}_i\}_{i=1}^{\tilde{m}} \rangle, \quad (10)$$

where $\tilde{m} = m_1 + m_2, \tilde{A} = \text{diag}(\Lambda, \Gamma) \in \mathbb{S}^{s_1+s_2}, \tilde{A}_i = \text{diag}(A_i, C_i) \in \mathbb{S}^{s_1+s_2}$ and

$$\tilde{B}^i = \begin{cases} \text{diag}(B_i, \mathbf{0}), & 1 \leq i \leq m_1 \\ \text{diag}(\mathbf{0}, D_{i-m_1}), & m_1+1 \leq i \leq \tilde{m} \end{cases}.$$

The computational complexity is $\mathcal{O}(1)$.

Proof: The expression of (10) directly follows from Definition 2 and [32, p. 428].

Complexity: Constructing \tilde{A}, \tilde{A}_i and \tilde{B}_i only involves matrix concatenation. ■

5) Cartesian Product: Then we introduce the Cartesian product for spectrahedral shadows.

Proposition 5 (Cartesian product): Given $\mathcal{S}_1 = \langle A, \{A_i\}_{i=1}^{n_1}, \{B_i\}_{i=1}^{m_1} \rangle$ with size s_1 and $\mathcal{S}_2 = \langle \Gamma, \{C_i\}_{i=1}^{n_2}, \{D_i\}_{i=1}^{m_2} \rangle$ with size s_2 , we have

$$\mathcal{S}_1 \times \mathcal{S}_2 = \langle \tilde{A}, \{\tilde{A}_i\}_{i=1}^{\tilde{n}}, \{\tilde{B}_i\}_{i=1}^{\tilde{m}} \rangle, \quad (11)$$

where $\tilde{n} = n_1 + n_2, \tilde{m} = m_1 + m_2, \tilde{A}, \tilde{A}_i, \tilde{B}_i \in \mathbb{S}^{s_1+s_2}, \tilde{A} = \text{diag}(\Lambda, \Gamma)$ and

$$\tilde{A}^i = \begin{cases} \text{diag}(A^i, \mathbf{0}), & 1 \leq i \leq n_1 \\ \text{diag}(\mathbf{0}, C^{i-n_1}), & n_1+1 \leq i \leq \tilde{n} \end{cases}$$

$$\tilde{B}^i = \begin{cases} \text{diag}(B^i, \mathbf{0}), & 1 \leq i \leq m_1 \\ \text{diag}(\mathbf{0}, D^{i-m_1}), & m_1+1 \leq i \leq \tilde{m} \end{cases}.$$

The computational complexity is $\mathcal{O}(1)$.

Proof: Assume that $x \in \mathcal{S}_1, u \in \mathcal{S}_2$ and $z = [x^T, u^T]^T$. Then it can be verified that $x \in \mathcal{S}_1$ and $u \in \mathcal{S}_2$ iff $\exists e \in \mathbb{R}^{\tilde{m}}, \tilde{A} + \sum_{i=1}^{\tilde{n}} z_i \tilde{A}_i + \sum_{i=1}^{\tilde{m}} e_i \tilde{B}_i \succeq 0$, which yields (11).

Complexity: Constructing \tilde{A}, \tilde{A}_i and \tilde{B}_i only involves matrix concatenation. ■

6) Minkowski-Firey L_p sum: Minkowski-Firey L_p sum is the concept first studied in Brunn-Minkowski-Firey theory for the mixed volumes problem [33]–[35]. Based on ellipsoids, recent work [3] introduced this set operation into RA. In the following part, we prove that spectrahedral shadows are closed under Minkowski-Firey L_p sum.

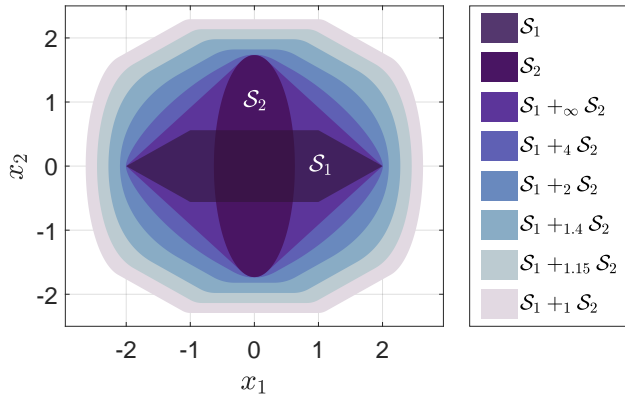


Fig. 2. Minkowski-Firey L_p -sums of a zonotope \mathcal{S}_1 and an ellipsoid \mathcal{S}_2 for $p \in \{1, 1.15, 1.4, 2, 4, \infty\}$.

Definition 2: Given $p \geq 1$ and $X, Y \subset \mathbb{R}^n$ with $\mathbf{0} \in X \cap Y$, the Minkowski-Firey L_p sum of X and Y is defined as

$$X +_p Y = \{t^{1/p'} x + (1-t)^{1/p'} y : x \in X, y \in Y, 0 \leq t \leq 1\}$$

where p' is the Hölder conjugate of p , i.e., $\frac{1}{p} + \frac{1}{p'} = 1$.

Remark 3: One might notice that Definition 2 is different from the classical definition of Minkowski-Firey L_p sum as defined by support functions, e.g., [33], [35]. Indeed, the classical definition is only valid for compact convex sets. It was shown in [36] that Definition 2 generalizes the classical definition to the case of arbitrary subsets in Euclidean space. In this paper, we adopt Definition 2 since spectrahedral shadows are not necessarily compact sets (see Example 1).

For sets containing the origin, the Minkowski sum and convex hull are two special cases of Minkowski-Firey L_p -sum when $p = 1$ and $p = \infty$, respectively. Moreover, the Minkowski-Firey L_p -sum of two sets X_1 and X_2 has the following inclusion relationship

$$X_1 +_1 X_2 \supseteq X_1 +_{p_1} X_2 \supseteq X_1 +_{p_2} X_2 \supseteq X_1 +_{\infty} X_2$$

for arbitrary $1 \leq p_1 \leq p_2 \leq \infty$ [33]. Fig 2 gives an example to illustrate the Minkowski-Firey L_p -sum of two sets with the increasing value of p . Then we introduce Lemma 5 as the prerequisite for the subsequent Proposition 6.

Lemma 5 ([37]): Given arbitrary rational q with $0 \leq q \leq 1$, the set $\{x \in \mathbb{R}^2 : x_1^q \geq x_2 \geq 0\}$ is exactly $\mathcal{S}(q) =$

$$\left\{ x \in \mathbb{R}^2 : \begin{bmatrix} \frac{t_j^{i-1} + t_j^{i-1}}{2} & 0 & t_j^i \\ * & \frac{t_{2j-1}^{i-1} + t_{2j}^{i-1}}{2} & \frac{t_{2j-1}^{i-1} - t_{2j}^{i-1}}{2} \\ * & * & \frac{t_{2j-1}^{i-1} + t_{2j}^{i-1}}{2} \end{bmatrix} \succeq 0, \forall 1 \leq i \leq l, \forall 1 \leq j \leq 2^{l-i} \right\}$$

where $c_1, c_2 \in \mathbb{N}$, $q = \frac{c_1}{c_2}$ is the fraction in lowest terms, and l is the smallest integer such that $2^l \geq c_2$.

Proof: By the construction technique in [37, Lecture 3.3.1], $\{x \in \mathbb{R}^2 : x_1^q \geq x_2 \geq 0\}$ is formulated as a conic quadratic-representable set. Then we obtain Lemma 5 using the well-known method to convert general conic quadratic-representable sets to spectrahedral shadows [37, (4.2.1)]. ■

In Lemma 5, all linear equations defining $\mathcal{S}(q)$ can be eliminated through variable substitution. Namely, $\mathcal{S}(q)$ is only defined by LMIs, which means that $\mathcal{S}(q)$ is a spectrahedral shadow. Due to space limitations and for the sake of clarity, we write $\mathcal{S}(q)$ in the form of Lemma 5 instead of Definition 2. In practice, once the value of p is determined, $\mathcal{S}(q)$ can be directly written as the form of Definition 2 according to Lemma 5.

Proposition 6 (Minkowski-Firey L_p sum): Given $\mathcal{S}_1 = \langle A, \{A_i\}_{i=1}^n, \{B_i\}_{i=1}^{m_1} \rangle$ with size s_1 , $\mathcal{S}_2 = \langle \Gamma, \{C_i\}_{i=1}^n, \{D_i\}_{i=1}^{m_2} \rangle$ with size s_2 , $\mathbf{0} \in \mathcal{S}_1 \cap \mathcal{S}_2$ and arbitrary rational p with $p \geq 1$, we have

$$\mathcal{S}_1 +_p \mathcal{S}_2 = \{x \in \mathbb{R}^n : \exists y \in \mathbb{R}^m, [y_1, y_3]^T, [y_2, y_4]^T \in \mathcal{S}(q) \\ \tilde{A} + \sum_{i=1}^n x_i \tilde{A}_i + \sum_{i=1}^m y_i \tilde{B}_i \succeq 0\}. \quad (12)$$

In (12), $m = n + m_1 + m_2 + 4$, $q = 1 - \frac{1}{p}$, $\mathcal{S}(q)$ is the spectrahedral shadow constructed by applying Lemma 5, and

$$\tilde{A} = \text{diag}\left(\begin{bmatrix} 1 & 0 \\ * & -1 \end{bmatrix}, \mathbf{0}\right),$$

$$\tilde{A}_i = \text{diag}(\mathbf{0}_{2 \times 2}, A_i, \mathbf{0}), \quad i = 1, 2, \dots, n,$$

$$\tilde{B}_i = \begin{cases} \text{diag}\left(\begin{bmatrix} -1 & 0 \\ * & 1 \end{bmatrix}, \mathbf{0}\right), & 1 \leq i \leq 2 \\ \text{diag}(\mathbf{0}_{2 \times 2}, \Lambda^+, \mathbf{0}), & i = 3 \\ \text{diag}(\mathbf{0}, \Gamma^+), & i = 4 \\ \text{diag}(\mathbf{0}, -A_{i-4}, C_{i-4}), & 5 \leq i \leq n+4 \\ \text{diag}(\mathbf{0}_{2 \times 2}, B_{i-n-4}, \mathbf{0}), & n+5 \leq i \leq n+m_1+4 \\ \text{diag}(\mathbf{0}, D_{i-n-m_1-4}), & n+m_1+5 \leq i \leq m \end{cases},$$

where $\tilde{A}, \tilde{A}_i, \tilde{B}_i \in \mathbb{S}^{2+s_1+s_2}$, and Λ^+ and Γ^+ are obtained by choosing $y^* \in \mathbb{R}^{m_1}$ and $v^* \in \mathbb{R}^{m_2}$ such that $\Lambda^+ = \Lambda + \sum_{i=1}^{m_1} y_i^* B_i \succeq 0$ and $\Gamma^+ = \Gamma + \sum_{i=1}^{m_2} y_i^* D_i \succeq 0$, respectively. The overall computational complexity is $\mathcal{O}(ns_1^2 + \sqrt{s_1}(m_1 s_1^2 + m_1^2 + s_1^2) + \sqrt{s_2}(m_2 s_2^2 + m_2^2 + s_2^2))$.

Proof: Due to $\mathbf{0} \in \mathcal{S}_1$, there always exists y^* such that $\Lambda^+ = \Lambda + \sum_{i=1}^{m_1} y_i^* B_i \succeq 0$, and

$$\exists y \in \mathbb{R}^m, \Lambda + \sum_{i=1}^n x_i A_i + \sum_{i=1}^m y_i B_i \succeq 0 \\ \xleftrightarrow{\tilde{y} = y - y^*} \exists \tilde{y} \in \mathbb{R}^m, \Lambda^+ + \sum_{i=1}^n x_i A_i + \sum_{i=1}^m \tilde{y}_i B_i \succeq 0,$$

which implies $\mathcal{S}_1 = \langle \Lambda^+, \{A_i\}_{i=1}^n, \{B_i\}_{i=1}^{m_1} \rangle$. Similarly, we have $\mathcal{S}_2 = \langle \Gamma^+, \{C_i\}_{i=1}^n, \{D_i\}_{i=1}^{m_2} \rangle$. For any $r \in \mathcal{S}_1 +_p \mathcal{S}_2$, there exists $x \in \mathcal{S}_1$ and $u \in \mathcal{S}_2$ such that

$$r = t_1^{1/p'} x + t_2^{1/p'} u, \quad \exists t_1, t_2 \geq 0, t_1 + t_2 = 1. \quad (13)$$

Let $\bar{x} = t_1^{1/p'} x$ and $\bar{u} = t_2^{1/p'} u$. It follows from (13) that $r \in \mathcal{S}_r$, where

$$\mathcal{S}_r = \left\{ \bar{x} + \bar{u} : \begin{aligned} & \exists \bar{y} \in \mathbb{R}^{m_1}, \bar{v} \in \mathbb{R}^{m_2}, t_1, t_2 \geq 0, t_1 + t_2 = 1 \\ & t_1^{1/p'} \Lambda^+ + \sum_{i=1}^n \bar{x}_i A_i + \sum_{i=1}^{m_1} \bar{y}_i B_i \succeq 0, \\ & t_2^{1/p'} \Gamma^+ + \sum_{i=1}^n \bar{u}_i C_i + \sum_{i=1}^{m_2} \bar{v}_i D_i \succeq 0 \end{aligned} \right\}.$$

Thus, $\mathcal{S}_1 +_p \mathcal{S}_2 \subseteq \mathcal{S}_r$. Note that the reverse of the above derivation (i.e., $\mathcal{S}_r \subseteq \mathcal{S}_1 +_p \mathcal{S}_2$) holds true as long as $t_1, t_2 \neq 0$. Consider the remaining case of $t_1 = 0$ (and hence $t_2 = 1$) without loss of generality. For arbitrary $\bar{r} \in \mathcal{S}_r$, there exists $\bar{x}, \bar{y}, \bar{u}, \bar{v}$ satisfying $\sum_{i=1}^n \bar{x}_i A_i + \sum_{i=1}^{m_1} \bar{y}_i B_i \succeq 0$ and $\Gamma^+ + \sum_{i=1}^n \bar{u}_i C_i + \sum_{i=1}^{m_2} \bar{v}_i D_i \succeq 0$ such that $\bar{r} = \bar{x} + \bar{u}$. Due to $\bar{x} \in \mathcal{S}_1$ (note $\Lambda^+ \succeq 0$), $\bar{u} \in \mathcal{S}_2$ and $t_2 = 1$, the condition (13) holds for \bar{r} , i.e., $\bar{r} \in \mathcal{S}_1 +_p \mathcal{S}_2$. Hence, $\mathcal{S}_r \subseteq \mathcal{S}_1 +_p \mathcal{S}_2$ also holds for $t_1 = 0$ or $t_2 = 0$. It follows from $\mathcal{S}_1 +_p \mathcal{S}_2 \subseteq \mathcal{S}_r$ that $\mathcal{S}_r = \mathcal{S}_1 +_p \mathcal{S}_2$. Due to $\Lambda^+, \Gamma^+ \succeq 0$, \mathcal{S}_r is equivalent to

$$\left\{ \begin{array}{l} \exists \bar{y} \in \mathbb{R}^{m_1}, \bar{v} \in \mathbb{R}^{m_2}, t_1 + t_2 = 1 \\ \bar{x} + \bar{u}: \begin{array}{l} t_3 \Lambda^+ + \sum_{i=1}^n \bar{x}_i A_i + \sum_{i=1}^{m_1} \bar{y}_i B_i \succeq 0, \\ t_4 \Gamma^+ + \sum_{i=1}^n \bar{u}_i C_i + \sum_{i=1}^{m_2} \bar{v}_i D_i \succeq 0, \\ t_1^{1/p'} \geq t_3 \geq 0, t_2^{1/p'} \geq t_4 \geq 0 \end{array} \end{array} \right\}. \quad (14)$$

Then (14) is written as (12) by analogy with Proposition 4.

Complexity: Constructing $\mathcal{S}(q)$ as a spectrahedral shadow by Lemma 5 only involves matrix element assignment, where the size of the matrix is constant once the value of q is determined. Hence, the complexity is $\mathcal{O}(c(q))$, where $c(q)$ is a constant about q . Moreover, Λ^+ and Γ^+ can be obtained by finding a feasible solution to an SDP problem, and the complexity is $\mathcal{O}(\sqrt{s_1}(m_1 s_1^2 + m_1^\omega + s_1^\omega) + \sqrt{s_2}(m_2 s_2^2 + m_2^\omega + s_2^\omega))$. The complexity to compute $-A_i$ for all $1 \leq i \leq n$ is $\mathcal{O}(n s_1^2)$. The remaining operation is matrix concatenation. Omitting constant and lower-order terms, the overall complexity is $\mathcal{O}(n s_1^2 + \sqrt{s_1}(m_1 s_1^2 + m_1^\omega + s_1^\omega) + \sqrt{s_2}(m_2 s_2^2 + m_2^\omega + s_2^\omega))$. ■

Remark 4: We can extend Proposition 6 to compute the Minkowski-Firey L_p sums of l spectrahedral shadows within $\mathcal{O}(n s_1^2 + \sum_{i=1}^l \sqrt{s_i}(m_i s_i^2 + m_i^\omega + s_i^\omega))$ time, where s_i and m_i are the size and lifted dimension of the i -th added spectrahedral shadow. In the literature, [3] proposes an outer approximated method to compute the Minkowski-Firey L_p sum of l n -dimensional ellipsoids within $\mathcal{O}(l n^3)$ time [3, Section VI-D]. We will see in Section III-C that n -dimensional ellipsoids are a special case of n -dimensional spectrahedral shadows with size $n+1$ and lifted dimension 0. This means that the task in [3] can be solved through Proposition 6 within $\mathcal{O}(n(n+1)^2 + \sum_{i=1}^l \sqrt{n+1}(n+1)^\omega) = \mathcal{O}(n^3 + l n^{\omega+0.5})$ runtime without approximation.

7) Conic hull: Then we introduce the *conic hull*, which is an operation commonly used in convex analysis and optimization.

Definition 3: Given $X \subset \mathbb{R}^n$, the *conic hull* of X is defined as $\text{cone}(X) = \{tx : x \in X, t \geq 0\}$.

Geometrically, the conic hull of a set X is the smallest cone that contains X . Fig. 3(a) shows an example of the conic hull of a spectrahedral shadows. Then Proposition 7 shows how to compute the conic hull of spectrahedral shadows.

Proposition 7 (Conic hull): For any nonempty $\mathcal{S} = \langle \Lambda, \{A_i\}_{i=1}^n, \{B_i\}_{i=1}^{m_1} \rangle$ with size s , there is a spectrahedral shadow $\mathcal{S}_c = \langle \mathbf{0}, \{A_i^c\}_{i=1}^n, \{B_i^c\}_{i=1}^{m_1+1} \rangle$ with

$$\begin{aligned} A_i^c &= \text{diag}(A_i, 0) \in \mathbb{S}^{s+1}, \forall 1 \leq i \leq n, \\ B_i^c &= \begin{cases} \text{diag}(B_i, \mathbf{0}), & 1 \leq i \leq m_1 \\ \text{diag}(\Lambda, 1), & i = m_1 + 1 \end{cases} \in \mathbb{S}^{s+1} \end{aligned} \quad (15)$$

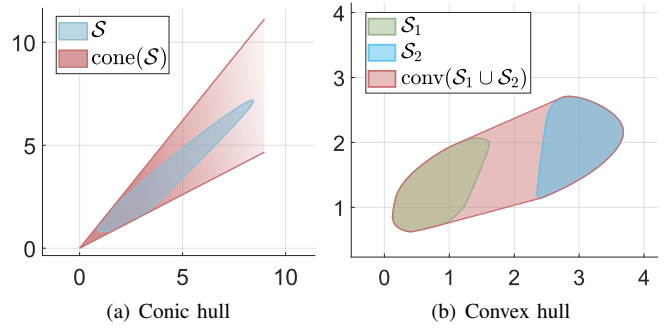


Fig. 3. The conic hull and convex hull of spectrahedral shadows.

such that

$$\text{cone}(\mathcal{S}) \subseteq \mathcal{S}_c, \quad \overline{\text{cone}(\mathcal{S})} = \overline{\mathcal{S}_c}. \quad (16)$$

Particularly, if $\mathbf{0} \in \mathcal{S}$ or \mathcal{S} is a bounded set, then

$$\text{cone}(\mathcal{S}) = \mathcal{S}_c. \quad (17)$$

The computational complexity to obtain \mathcal{S}_c is $\mathcal{O}(1)$.

Proof: \mathcal{S}_c can be rewritten as

$$\{x \in \mathbb{R}^n : \exists y \in \mathbb{R}^m, t \geq 0, t\Lambda + \sum_{i=1}^n x_i A_i + \sum_{i=1}^m y_i B_i \succeq 0\}.$$

Similar to the proof of $\mathcal{S}_1 +_p \mathcal{S}_2 \subseteq \mathcal{S}_r$ in Proposition 6, we obtain $\text{cone}(\mathcal{S}) \subseteq \mathcal{S}_c$. Then we prove $\overline{\text{cone}(\mathcal{S})} = \overline{\mathcal{S}_c}$. Since $\text{cone}(\mathcal{S}) \subseteq \mathcal{S}_c$, we only need to prove $\mathcal{S}_c \subseteq \overline{\text{cone}(\mathcal{S})}$. For any $r \in \mathcal{S}_c$, there exist $y \in \mathbb{R}^m$ and $t \geq 0$ such that $t\Lambda + \sum_{i=1}^n r_i A_i + \sum_{i=1}^m y_i B_i \succeq 0$. Let $r^\epsilon = r + \epsilon r$, $t^\epsilon = t + \epsilon t$ and $y^\epsilon = y + \epsilon y$ with $\epsilon > 0$. It is clear that $t^\epsilon > 0$ and $t^\epsilon \Lambda + \sum_{i=1}^n r_i^\epsilon A_i + \sum_{i=1}^m y_i^\epsilon B_i \succeq 0$. Then there exist $x^\epsilon = \frac{r^\epsilon}{t^\epsilon}$ and $\tilde{y}^\epsilon = \frac{y^\epsilon}{t^\epsilon}$ satisfying $\Lambda + \sum_{i=1}^n x_i^\epsilon A_i + \sum_{i=1}^m \tilde{y}_i^\epsilon B_i \succeq 0$, which implies $x^\epsilon \in \mathcal{S}$ and hence we have $r^\epsilon \in \text{cone}(\mathcal{S})$ according to Definition 3. When $\epsilon \rightarrow +0$, we have $r_\epsilon \rightarrow r$, and $r \in \overline{\text{cone}(\mathcal{S})}$ holds due to the closure property of $\overline{\text{cone}(\mathcal{S})}$. Thus, $\mathcal{S}_c \subseteq \overline{\text{cone}(\mathcal{S})}$.

Consider the case of $\mathbf{0} \in \mathcal{S}$. By analogy with the proof of $\mathcal{S}_r \subseteq \mathcal{S}_1 +_p \mathcal{S}_2$ in Proposition 6, we have $\mathcal{S}_c \subseteq \text{cone}(\mathcal{S})$, thereby leading to (17). Then consider the case where \mathcal{S} is bounded. For arbitrary $r \in \mathcal{S}_c$, there exist $y \in \mathbb{R}^m$ and $t \geq 0$ such that $t\Lambda + \sum_{i=1}^n r_i A_i + \sum_{i=1}^m y_i B_i \succeq 0$. When $t > 0$, we have $r \in \text{cone}(\mathcal{S})$ by variable substitution. To prove $r \in \text{cone}(\mathcal{S})$ for $t = 0$, let $x^r = x^* + \alpha r$ with $\alpha \geq 0$ and $x^* \in \mathcal{S}$. It follows from $\sum_{i=1}^n r_i A_i + \sum_{i=1}^m y_i B_i \succeq 0$ and $\exists y^* \in \mathbb{R}^m, \Lambda + \sum_{i=1}^n x_i^* A_i + \sum_{i=1}^m y_i^* B_i \succeq 0$ that $\exists y^r = y^* + \alpha y, \Lambda + \sum_{i=1}^n x_i^r A_i + \sum_{i=1}^m y_i^r B_i \succeq 0$, i.e., $x^r \in \mathcal{S}$. If $r \neq \mathbf{0}$, it is contradictory to state that \mathcal{S} is bounded, given that

$$\lim_{\alpha \rightarrow +\infty} x^* + \alpha r = \lim_{\alpha \rightarrow +\infty} x^r \in \mathcal{S}.$$

Thus, $r = \mathbf{0} \in \text{cone}(\mathcal{S})$ and we finally obtain $\mathcal{S}_c \subseteq \text{cone}(\mathcal{S})$.

Complexity: Constructing (15) only needs matrix concatenation. ■

Remark 5: A special case of Proposition 7, i.e., computing the closed conic hull of $\langle \Lambda, \{A_i\}_{i=1}^n, \{B_i\}_{i=1}^{m_1} \rangle$ under the implication condition $\sum_{i=1}^m y_i B_i \succeq 0 \Rightarrow y = \mathbf{0}$, is given in [32, p. 428]. Moreover, from the perspective of convex

analysis, \mathcal{S}_c given in Proposition 7 is not the exact conic hull of \mathcal{S} when the condition for (17) is invalid. But in practice, \mathcal{S}_c can be seen as the lossless conic hull of \mathcal{S} even if the condition for (17) is invalid, because \mathcal{S}_c and $\text{cone}(\mathcal{S})$ have the same interior and differ at most on the topological boundaries (see (16)). The same is true for the following convex hull and polytopic map computation.

8) Convex hull: Besides the conic hull, the *convex hull* is also commonly seen in convex analysis and optimization. The problem of computing the convex hull of spectrahedral shadows has been addressed in [16]. Here we introduce the expression as the following Lemma 6.

Lemma 6 (Convex hull, [16, Theorem 2.2]): For arbitrary nonempty $\mathcal{S}_1 = \langle \Lambda^1, \{A_i\}_{i=1}^n, \{B_i\}_{i=1}^{m_1} \rangle$ with size s_1 and $\mathcal{S}_2 = \langle \Lambda^2, \{C_i\}_{i=1}^n, \{D_i\}_{i=1}^{m_2} \rangle$ with size s_2 , there is a spectrahedral shadow $\mathcal{S}_v = \langle \Lambda^v, \{A_i^v\}_{i=1}^n, \{B_i^v\}_{i=1}^{m_v} \rangle$ with

$$\begin{aligned} \Lambda^v &= \text{diag}\left(\begin{bmatrix} 1 & 0 \\ * & 0 \end{bmatrix}, \mathbf{0}, \Lambda^2\right), \\ A_i^v &= \text{diag}(\mathbf{0}, C_i), \quad i = 1, 2, \dots, n, \\ B_i^v &= \begin{cases} \text{diag}\left(\begin{bmatrix} -1 & 0 \\ * & 1 \end{bmatrix}, \Lambda^1, -\Lambda^2\right), & i = 1 \\ \text{diag}(\mathbf{0}, A_{i-1}, -C_{i-1}), & 2 \leq i \leq n+1 \\ \text{diag}(\mathbf{0}_{2 \times 2}, B_{i-n-1}, \mathbf{0}), & n+2 \leq i \leq n+m_1+1 \\ \text{diag}(\mathbf{0}, D_{i-n-m_1-1}), & n+m_1+2 \leq i \leq m \end{cases}, \end{aligned}$$

such that

$$\text{conv}(\mathcal{S}_1 \cup \mathcal{S}_2) \subseteq \mathcal{S}_v, \quad \overline{\text{conv}(\mathcal{S}_1 \cup \mathcal{S}_2)} = \overline{\mathcal{S}_v}, \quad (18)$$

where $\Lambda^v, A_i^v, B_i^v \in \mathbb{S}^{2+s_1+s_2}$ and $m = n + m_1 + m_2 + 1$. Particularly, if \mathcal{S}_1 and \mathcal{S}_2 are both bounded sets, then

$$\text{conv}(\mathcal{S}_1 \cup \mathcal{S}_2) = \mathcal{S}_v. \quad (19)$$

The computational complexity to obtain \mathcal{S}_v is $\mathcal{O}(ns_2^2)$.

Proof: The expression of \mathcal{S}_v follows from [16, Theorem 2.2] and Proposition 4.

Complexity: Computing $-\Lambda^2$ and $-C_i$ for all $1 \leq i \leq n$ has complexity $\mathcal{O}(s_2^2)$ and $\mathcal{O}(ns_2^2)$, respectively. The remaining operation is matrix concatenation, and hence the overall complexity is $\mathcal{O}(ns_2^2)$. ■

9) Linear set-valued map: To propagate uncertainties on uncertain LPV systems, spectrahedral shadows should be able to represent the sets under *linear set-valued maps*. Intuitively, a set-valued map maps a point into a set. We give a formal statement of the linear set-valued map in Definition 4.

Definition 4 (Linear set-valued map): A set-valued function $\mathbf{T} : \mathbb{R}^n \rightarrow \mathbb{P}(\mathbb{R}^n)$ is called a *linear set-valued map* if $\mathbf{T}(x+y) = \mathbf{T}(x) \oplus \mathbf{T}(y)$ and $\mathbf{T}(cx) = c\mathbf{T}(x)$ for all $x, y \in \mathbb{R}^n$ and $c \in \mathbb{R}$. A set $X \subset V$ under a linear set-valued map \mathbf{T} is defined as $\mathbf{T}(X) = \bigcup_{x \in X} \mathbf{T}(x)$.

The linear set-valued map can be further classified based on the type of the set $\mathbf{T}(x)$, e.g., interval map [7], [9] ($\mathbf{T}(x)$ is an interval) and polytopic map ($\mathbf{T}(x)$ is a polytope). Next, we derive the expression of spectrahedral shadows under the polytopic map, and the polytopic map is the common form

of linear set-valued map on uncertain LPV systems (e.g., [5], [20]).

Proposition 8 (Polytopic map): For $T_1, T_2, \dots, T_h \in \mathbb{R}^{l \times n}$, $\mathbf{T} = \text{conv}\{T_1, T_2, \dots, T_h\} \subset \mathbb{R}^{l \times n}$ and $\mathcal{S} = \langle \Lambda, \{A_i\}_{i=1}^n, \{B_i\}_{i=1}^{m_p} \rangle$ with size s , there is a spectrahedral shadows $\mathcal{S}_p = \langle \Lambda^p, \{A_i^p\}_{i=1}^l, \{B_i^p\}_{i=1}^{m_p} \rangle$ with

$$\begin{aligned} \Lambda^p &= \text{diag}(\mathbf{0}, \begin{bmatrix} 1 & 0 \\ * & -1 \end{bmatrix}), \\ A_i^p &= \text{diag}(A_i^1, \mathbf{0}), \quad i = 1, 2, \dots, l, \\ \{B_i^p\}_{i=1}^{m_p} &= \{M_1, \dots, M_h, N_1^2, \dots, N_l^2, N_1^3, \dots, N_l^3, \dots, N_l^h, \\ &\quad O_1^1, \dots, O_{m_1}^1, O_1^2, \dots, O_{m_2}^2, \dots, O_{m_h}^h\} \end{aligned}$$

such that

$$\mathbf{T}(\mathcal{S}) \subseteq \mathcal{S}_p, \quad \overline{\mathbf{T}(\mathcal{S})} = \overline{\mathcal{S}_p}, \quad (20)$$

where $\Lambda^p, A_i^p, B_i^p \in \mathbb{S}^{s_p}$, $s_p = 2 + h + \sum_{i=1}^h s_i$, $m_p = h + l(h-1) + \sum_{i=1}^h m_i$, s_i is the corresponding size of $\langle \Lambda^i, \{A_j^i\}_{j=1}^l, \{B_j^i\}_{j=1}^{m_i} \rangle$ ($1 \leq i \leq h$), and

$$\begin{aligned} \langle \Lambda^i, \{A_j^i\}_{j=1}^l, \{B_j^i\}_{j=1}^{m_i} \rangle &= T_i \circ \mathcal{S}, \quad \forall 1 \leq i \leq h, \\ M_i &= \text{diag}\left(\underbrace{0, \dots, 0}_{i-1}, 1, \underbrace{0, \dots, 0}_{h-i+\sum_{k=1}^h s_k}, -1, 1\right), \quad \forall 1 \leq i \leq h, \\ N_j^i &= \text{diag}\left(-A_j^1, \underbrace{0, \dots, 0}_{\sum_{k=2}^{i-1} s_k}, A_j^i, \underbrace{0, \dots, 0}_{2+h+\sum_{k=i+1}^h s_k}\right), \quad \forall 2 \leq i \leq h, \\ &\quad \forall 1 \leq j \leq l, \\ O_j^i &= \text{diag}\left(\underbrace{0, \dots, 0}_{\sum_{k=1}^{i-1} s_k}, B_j^i, \underbrace{0, \dots, 0}_{2+h+\sum_{k=i+1}^h s_k}\right), \quad \forall 1 \leq i \leq h, \\ &\quad \forall 1 \leq j \leq m_i. \end{aligned}$$

Particularly, if $\mathbf{0} \in \mathcal{S}$ or \mathcal{S} is a bounded set, then

$$\mathbf{T}(\mathcal{S}) = \mathcal{S}_p. \quad (21)$$

The complexity to obtain \mathcal{S}_p is $\mathcal{O}(h\tilde{l}^4 + h\tilde{l}^3s + h\tilde{l}^2s^2)$, where $\tilde{l} = \max\{l, n\}$.

Proof: We first prove that $\mathbf{T}(\mathcal{S}) = \text{conv}(\bigcup_{i=1}^h T_i \circ \mathcal{S})$ by noticing $\mathbf{T} = \text{conv}\{T_1, T_2, \dots, T_h\}$ and

$$\begin{aligned} z \in \mathbf{T}(\mathcal{S}) &\Leftrightarrow z = \mathbf{T}(x), \exists x \in \mathcal{S} \Leftrightarrow z = Tx, \exists T \in \mathbf{T}, x \in \mathcal{S} \\ &\Leftrightarrow z = \sum_{i=1}^h \theta_i (T_i x), \exists \theta_i \geq 0, \sum_{i=1}^h \theta_i = 1, x \in \mathcal{S} \\ &\Leftrightarrow z \in \text{conv}(\bigcup_{i=1}^h T_i \circ \mathcal{S}). \end{aligned}$$

Denote $\mathcal{S}_i^T = T_i \circ \mathcal{S} = \langle \Lambda^i, \{A_j^i\}_{j=1}^l, \{B_j^i\}_{j=1}^{m_i} \rangle$. Then \mathcal{S}_i^T can be computed by Proposition 1. According to the convex hull expression given in [16, Theorem 2.2], there is a set

$$\mathcal{S}_p = \left\{ \sum_{i=1}^h u^i : \begin{aligned} &\exists v^i \in \mathbb{R}^{m_i}, t \in \mathbb{R}^h, t_i \geq 0, \sum_{i=1}^h t_i = 1 \\ &t_1 \Lambda^1 + \sum_{i=1}^l u_i^1 A_i^1 + \sum_{i=1}^{m_1} v_i^1 B_i^1 \succeq 0, \\ &t_2 \Lambda^2 + \sum_{i=1}^l u_i^2 A_i^2 + \sum_{i=1}^{m_2} v_i^2 B_i^2 \succeq 0, \\ &\vdots \\ &t_h \Lambda^h + \sum_{i=1}^l u_i^h A_i^h + \sum_{i=1}^{m_h} v_i^h B_i^h \succeq 0 \end{aligned} \right\}.$$

such that $T(\mathcal{S}) = \text{conv}(\cup_{i=1}^h \mathcal{S}_i^T) \subseteq \mathcal{S}_p$, $\overline{T(\mathcal{S})} = \overline{\mathcal{S}_p}$, and $T(\mathcal{S}) = \mathcal{S}_p$ when \mathcal{S}_i^T for $1 \leq i \leq h$ are all bounded. Due to $\mathcal{S}_i^T = T_i \circ \mathcal{S}$, the boundedness condition for all \mathcal{S}_i^T can be simplified as the boundedness for \mathcal{S} . For the case of $\mathbf{0} \in \mathcal{S}$, we have $\mathbf{0} \in \mathcal{S}_i^T$, then we can also prove $T(\mathcal{S}) = \mathcal{S}_p$ by analogy with the proof of Proposition 6. Let $x = \sum_{i=1}^h u^i \in \mathbb{R}^l$. Then \mathcal{S}_p is equivalently written as

$$\mathcal{S}_p = \left\{ x: \begin{array}{l} \exists t \in \mathbb{R}^h, u^2, u^3, \dots, u^h \in \mathbb{R}^l, v^i \in \mathbb{R}^{m_i}, 1 \leq i \leq h \\ A^p + \sum_{i=1}^n x_i A_i^p + \sum_{i=1}^h t_i M_i \\ + \sum_{i=2}^h \sum_{j=1}^l u_j^i N_j^i + \sum_{i=1}^h \sum_{j=1}^{m_i} v_j^i O_j^i \succeq 0 \end{array} \right\},$$

which yields Proposition 8.

Complexity: According to Proposition 1, computing $\langle A^i, \{A_j^i\}_{j=1}^l, \{B_j^i\}_{j=1}^{m_i} \rangle$ for $1 \leq i \leq h$ has $\mathcal{O}(hl^4 + hl^3s + hl^2s^2)$ complexity. The complexity of all other operations is a lower-order term, and hence the overall complexity is $\mathcal{O}(hl^4 + hl^3s + hl^2s^2)$. ■

B. Set Validations

In this section, we introduce the necessary set validations in SE, RA, and FD for spectrahedral shadows.

1) Emptiness Check: For RA and FD, it is common to test whether two sets intersect (i.e., the intersection of the sets is empty), such as collision check [12] and set separation [38]. Proposition 9 shows how to check the emptiness for spectrahedral shadows.

Proposition 9 (Emptiness Check): For arbitrary $\mathcal{S} = \langle A, \{A_i\}_{i=1}^n, \{B_i\}_{i=1}^m \rangle$ with size s , $\mathcal{S} = \emptyset$ iff $\epsilon_e^* < 0$, and ϵ^* is obtained by solving

$$\epsilon_e^* = \max_{\epsilon, x, y} \epsilon \quad \text{s.t.}, A + \sum_{i=1}^n x_i A_i + \sum_{i=1}^m y_i B_i \succeq \epsilon I, \quad (22)$$

where $x \in \mathbb{R}^n$ and $y \in \mathbb{R}^m$. The complexity to test whether \mathcal{S} is an empty set is $\mathcal{O}(\sqrt{s}((n+m)s^2 + (n+m)^\omega + s^\omega))$.

Proof: Let $\Lambda(x, y) = A + \sum_{i=1}^n x_i A_i + \sum_{i=1}^m y_i B_i$. According to Definition 2, $\mathcal{S} = \emptyset$ iff $\nexists x \in \mathbb{R}^n, y \in \mathbb{R}^m, \Lambda(x, y) \succeq 0$, which is further equivalent to $\max_{x, y} \lambda_{\min}(\Lambda(x, y)) < 0$. Then $\max_{x, y} \lambda_{\min}(\Lambda(x, y))$ is obtained by the well-known method to minimize the spectral norm, i.e., solving the SDP problem (22).

Complexity: Solving the SDP problem (22) runs in $\mathcal{O}(\sqrt{s}((n+m+1)s^2 + (n+m+1)^\omega + s^\omega))$ time. The complexity of comparing ϵ^* with 0 is $\mathcal{O}(1)$. By omitting the lower-order term, the overall complexity is $\mathcal{O}(\sqrt{s}((n+m)s^2 + (n+m)^\omega + s^\omega))$. ■

2) Point Containment: Point containment is a basic task in FD, since it needs to check whether the real system output lies in the output set of a healthy system [5]. We thus introduce Corollary 2 to validate this point for spectrahedral shadows.

Corollary 2 (Point Containment): For arbitrary $v \in \mathbb{R}^n$ and $\mathcal{S} = \langle A, \{A_i\}_{i=1}^n, \{B_i\}_{i=1}^m \rangle$ with size s , $v \in \mathcal{S}$ iff $\epsilon_p^* \geq 0$, and ϵ^* is obtained by solving

$$\epsilon_p^* = \max_{\epsilon, y} \epsilon \quad \text{s.t.}, A^v + \sum_{i=1}^m y_i B_i \succeq \epsilon I, \quad (23)$$

where $A^v = A + \sum_{i=1}^n v_i A_i$ and $y \in \mathbb{R}^m$. The complexity to test whether x_t lies in \mathcal{S} is $\mathcal{O}(ns^2 + \sqrt{s}(ms^2 + m^\omega + s^\omega))$.

Proof: Corollary 2 follows from Proposition 9 by noticing that $v \in \mathcal{S} \Leftrightarrow \langle A^v, \{B_i\}_{i=1}^m \rangle \neq \emptyset$ and the complexity of computing A^v is $\mathcal{O}(2ns^2)$. ■

3) Boundedness Check: In practice, not all sets are bounded, such as consistent state sets [9] and unguaranteed detectable faults sets [21]. Thus, a numerical method is proposed to check the boundedness of spectrahedral shadows.

Proposition 10 (Boundedness Check): For any nonempty $\mathcal{S} = \langle A, \{A_i\}_{i=1}^n, \{B_i\}_{i=1}^m \rangle$ with size s , \mathcal{S} is bounded iff $\text{rank}(P) = n$, $\text{rank}(P) + \text{rank}(Q) = \text{rank}([P, Q])$ and either of the following conditions holds

- 1) $\text{tr}(A_i) = 0, \forall 1 \leq i \leq n$ and $\text{tr}(B_j) = 0, \forall 1 \leq j \leq m$;
- 2) $\epsilon_b^* < 0$,

where $P = [\text{tvec}(A_1), \text{tvec}(A_2), \dots, \text{tvec}(A_n)] \in \mathbb{R}^{s(s+1)/2 \times n}$, $Q = [\text{tvec}(B_1), \text{tvec}(B_2), \dots, \text{tvec}(B_m)] \in \mathbb{R}^{s(s+1)/2 \times m}$, and ϵ_b^* is obtained by solving

$$\epsilon_b^* = \max_{\epsilon, x, y} \epsilon \quad (24a)$$

$$\text{s.t.}, \sum_{i=1}^n x_i A_i + \sum_{i=1}^m y_i B_i \succeq \epsilon I, \quad (24b)$$

$$\sum_{i=1}^n \text{tr}(A_i) x_i + \sum_{i=1}^m \text{tr}(B_i) y_i = 1. \quad (24c)$$

The complexity to test whether \mathcal{S} is bounded is $\mathcal{O}((m+n)s^4 + \sqrt{s}(m+n)^\omega)$.

Proof: We first prove that \mathcal{S} is unbounded iff $\exists u \in \mathbb{R}^n \setminus \{\mathbf{0}\}, v \in \mathbb{R}^m, \sum_{i=1}^n u_i A_i + \sum_{i=1}^m v_i B_i \succeq 0$. The sufficiency is clear by verifying $\lim_{\alpha \rightarrow \infty} x + \alpha u \in \mathcal{S}$ for $\forall x \in \mathcal{S}$, where $\alpha \in \mathbb{R}$. For the necessity, consider arbitrary $x \in \mathcal{S}$. Since \mathcal{S} is unbounded, there exists $d \in \mathbb{R}^n \setminus \{\mathbf{0}\}$ such that $x^\alpha = x + \alpha d \in \mathcal{S}$ holds for all $\alpha \geq 0$. Let $u^\alpha = \frac{x^\alpha}{\|x^\alpha\|}$ and $u^\infty = \lim_{\alpha \rightarrow +\infty} u^\alpha$. We have

$$\exists y \in \mathbb{R}^m, \frac{1}{\|x^\alpha\|} A + \sum_{i=1}^n u_i^\alpha A_i + \sum_{i=1}^m \frac{y_i}{\|x^\alpha\|} B_i \succeq 0, \quad (25)$$

which yields $\exists v = \frac{y}{\|x^\alpha\|}, \sum_{i=1}^n u_i^\alpha A_i + \sum_{i=1}^m v_i B_i \succeq 0$. Since $u^\alpha \in \mathcal{S} = \{x \in \mathbb{R}^n : \|x\| = 1\}$ and \mathcal{S} is a closed set, we have $u^\infty \in \mathcal{S} \subset \mathbb{R}^n \setminus \{\mathbf{0}\}$, thereby leading to the necessity.

Then consider Proposition 10 in three cases. For the case of $\text{rank}(P) < n$, we know $\exists u^* \in \mathbb{R}^n \setminus \{\mathbf{0}\}, Pu^* = \mathbf{0}$, which is equivalent to $\sum_{i=1}^n u_i^* A_i = \mathbf{0}$. Since $\exists v = \mathbf{0}, \sum_{i=1}^n u_i^* A_i + \sum_{i=1}^m v_i B_i \succeq 0$, \mathcal{S} is unbounded.

For the second case, i.e., $\text{rank}(P) = n$ and $\text{rank}(P) + \text{rank}(Q) < \text{rank}([P, Q])$, let $\mathcal{R}_P = \{\sum_{i=1}^n x_i P_{[i,*]} : x \in \mathbb{R}^n\}$ and $\mathcal{R}_Q = \{\sum_{i=1}^m x_i Q_{[i,*]} : x \in \mathbb{R}^m\}$ be the *range* of P and Q , respectively. Then $\text{rank}(P) + \text{rank}(Q) < \text{rank}([P, Q])$ is equivalent to $\dim(\mathcal{R}_P) + \dim(\mathcal{R}_Q) < \dim(\mathcal{R}_P \oplus \mathcal{R}_Q)$. By subspace intersection lemma [39, (0.1.7.1)], we have $\dim(\mathcal{R}_P \cap \mathcal{R}_Q) = \dim(\mathcal{R}_P \oplus \mathcal{R}_Q) - (\dim(\mathcal{R}_P) + \dim(\mathcal{R}_Q)) > 0$, i.e., $\mathcal{R}_P \cap \mathcal{R}_Q \not\subseteq \{\mathbf{0}\}$. Since P is full column rank, $\mathcal{R}_P \cap \mathcal{R}_Q \not\subseteq \{\mathbf{0}\}$ iff $\exists x \in \mathbb{R}^n \setminus \{\mathbf{0}\}, y \in \mathbb{R}^m, \sum_{i=1}^n x_i P_{[i,*]} = \sum_{i=1}^m y_i Q_{[i,*]}$. Let $u = x$ and $v = -y$. We have $\sum_{i=1}^n u_i A_i + \sum_{i=1}^m v_i B_i = \mathbf{0} \succeq 0$, and hence \mathcal{S} is unbounded.

For the third case, i.e., $\text{rank}(Q) = n$ and $\text{rank}(P) + \text{rank}(Q) = \text{rank}([P, Q])$, it can be concluded that $\nexists u \in \mathbb{R}^n \setminus \{\mathbf{0}\}$, $v \in \mathbb{R}^m$, $\sum_{i=1}^n u_i A_i + \sum_{i=1}^m v_i B_i = \mathbf{0}$ by analogy with the second case. Consider the subspace $\mathcal{R}_{AB} = \{\sum_{i=1}^n x_i A_i + \sum_{i=1}^m y_i B_i : x \in \mathbb{R}^n, y \in \mathbb{R}^m\}$ and denote $\mathbb{S}_+^n = \{X \in \mathbb{S}^n : X \succeq 0\}$. In this case, \mathcal{S} is unbounded (i.e., $\exists u \in \mathbb{R}^n \setminus \{\mathbf{0}\}$, $v \in \mathbb{R}^m$, $\sum_{i=1}^n u_i A_i + \sum_{i=1}^m v_i B_i \succeq 0$) iff $\mathcal{R}_{AB} \cap \mathbb{S}_+^n \not\subseteq \{\mathbf{0}\}$. Notice that both \mathcal{R}_{AB} and \mathbb{S}_+^n are cones in \mathbb{S}^n , $\mathcal{R}_{AB} \cap \mathbb{S}_+^n$ is a cone in \mathbb{S}_+^n , and hence

$$\begin{aligned} \mathcal{R}_{AB} \cap \mathbb{S}_+^n \not\subseteq \{\mathbf{0}\} &\Leftrightarrow (\mathcal{R}_{AB} \cap \mathbb{S}_+^n) \cap \text{spx}(n) \neq \emptyset \\ &\Leftrightarrow \mathcal{R}_{AB} \cap \text{spx}(n) \neq \emptyset, \end{aligned} \quad (26)$$

where $\text{spx}(n) = \{X \in \mathbb{S}_+^n : \text{tr}(X) = 1\}$ is the *spectraplex* (i.e., the generalization of simplex in \mathbb{S}^n). Then $\mathcal{R}_{AB} \cap \text{spx}(n) \neq \emptyset$ can be validated by analogy with Proposition 9, thereby leading to Proposition 10 (Note that the problem (24) is infeasible when $\text{tr}(A^i) = 0, \forall 1 \leq i \leq n$ and $\text{tr}(B_j) = 0, \forall 1 \leq j \leq m$, and hence $\mathcal{R}_{AB} \cap \text{spx}(n) = \emptyset$).

Complexity: When $s(s+1)/2 < n$, \mathcal{S} is clearly unbounded due to $\text{rank}(P) < n$. When $s(s+1)/2 \geq n$, the complexity to compute $\text{rank}(P)$, $\text{rank}(Q)$ and $\text{rank}([P, Q])$ using SVD is $\mathcal{O}(2(m+n)s^4)$, and the complexity to solve the SDP problem (24) is $\mathcal{O}(\sqrt{s}((m+n)s^2 + (m+n)\omega + s^\omega))$. Since the complexity of all other operations is a lower-order term, the overall complexity is reduced as $\mathcal{O}((m+n)s^4 + \sqrt{s}(m+n)\omega)$ by recalling $\omega \leq 2.372$. ■

C. Conversion from Existing Set Representations

In this section, we discuss some existing convex set representations that can be formulated as spectrahedral shadows.

1) H-polyhedron: We first show how to convert H-polyhedrons into spectrahedrons.

Lemma 7 (Conversion from H-polyhedrons): Given an H-polyhedron $\mathcal{P}(A, b) = \{x \in \mathbb{R}^n : Ax \leq b\}$ with $A \in \mathbb{R}^{m \times n}$ and $b \in \mathbb{R}^m$, \mathcal{P} can be represented by a spectrahedron $\langle \Lambda, \{A_i\}_{i=1}^n \rangle$ with size m , where $\Lambda = \text{diag}(b_1, b_2, \dots, b_m)$ and $A_i = \text{diag}(-A_{[1,i]}, -A_{[2,i]}, \dots, -A_{[m,i]})$, $\forall 1 \leq i \leq n$.

Proof: It is clear to formulate $\mathcal{P}(A, b)$ as $\langle \Lambda, \{A_i\}_{i=1}^n \rangle$ according to Definition 2. ■

2) Ellipsoid: Ellipsoids can also be readily represented as spectrahedral shadows.

Lemma 8 (Conversion from Ellipsoids): Given an ellipsoid $\mathcal{E}(c, Q) = \{x \in \mathbb{R}^n : (x - c)^T Q^{-1} (x - c) \leq 1, Q \succ 0\}$ with $Q \in \mathbb{S}^n$ and $c \in \mathbb{R}^n$, $\mathcal{E}(c, Q)$ can be represented by a spectrahedron $\langle \Lambda, \{A_i\}_{i=1}^n \rangle$ with size $n+1$, where

$$\Lambda = \begin{bmatrix} Q & -c \\ -c^T & 1 \end{bmatrix}, \quad A_{[j,k]}^i = \begin{cases} 1, & j = n+i, k = 1 \\ 1, & j = 1, k = n+i, \forall 1 \leq i \leq n \\ 0, & \text{otherwise} \end{cases}$$

Proof: By Schur complement lemma, $(x - c)^T Q^{-1} (x - c) \leq 1$ and $Q \succ 0$ iff $\begin{bmatrix} Q & x - c \\ (x - c)^T & 1 \end{bmatrix} \succeq 0$, which yields Proposition 8. ■

3) Zonotope: Then we show how to convert zonotopes into spectrahedral shadows based on the developed set operations.

Proposition 11 (Conversion from Zonotopes): Given a zonotope $\mathcal{Z}(c, G) = \{x \in \mathbb{R}^n : x = c + G\xi, \|\xi\|_\infty \leq 1\}$ with $c \in \mathbb{R}^n$ and $G \in \mathbb{R}^{n \times n_g}$, $\mathcal{Z}(c, G)$ can be represented by a spectrahedral shadow $\langle \Lambda, \{A_i\}_{i=1}^n, \{B_i\}_{i=1}^{n_g-r_g} \rangle$ with size $2(n + n_g - r_g)$, where $r_g = \text{rank}(G)$, $G = UDV^T$ is the SVD of G , G^\dagger is the Moore-Penrose inverse of G , and

$$\begin{aligned} \Lambda &= \text{diag}(I_{2n_g}, \mathbf{0}) - \sum_{i=1}^n c_i A_i, \\ A_i &= \text{diag}(G_{[1,i]}^\dagger, G_{[2,i]}^\dagger, \dots, G_{[n_g,i]}^\dagger, -G_{[1,i]}^\dagger, -G_{[2,i]}^\dagger, \dots, \\ &\quad -G_{[n_g,i]}^\dagger, U_{[r_g+1,i]}, U_{[r_g+2,i]}, \dots, U_{[n,i]}, \\ &\quad -U_{[r_g+1,i]}, -U_{[r_g+2,i]}, \dots, -U_{[n,i]}), \forall 1 \leq i \leq n, \\ B_i &= \text{diag}(V_{[1,r_g+i]}, V_{[2,r_g+i]}, \dots, V_{[n_g,r_g+i]}, -V_{[1,r_g+i]}, \\ &\quad -V_{[2,r_g+i]}, \dots, -V_{[n_g,r_g+i]}), \forall 1 \leq i \leq n_g - r_g. \end{aligned}$$

Proof: $\mathcal{Z}(c, G)$ can be rewritten as $c + G \circ \mathcal{B}_\infty^{n_g}$, where the unit ∞ -norm ball $\mathcal{B}_\infty^{n_g}$ is represented by the H-polyhedron $\{x \in \mathbb{R}^{n_g} : [I_{n_g}, -I_{n_g}]^T x \leq \mathbf{1}\}$. Using Lemma 7, $\mathcal{B}_\infty^{n_g}$ can be further formulated as a spectrahedral shadow. Due to $\mathcal{Z}(c, G) = c + G \circ \mathcal{B}_\infty^{n_g}$, $\mathcal{Z}(c, G)$ is formulated as a spectrahedral shadow by Propositions 1 and 2. ■

4) Ellipsoid & Constrained Zonotope: For more complex set representations like ellipsotopes, we provide an algorithm to convert them into spectrahedral shadows. This algorithm is equally applicable for constrained zonotopes, as they are readily written as ellipsotopes [12, Section IV-E]

The basic idea of the algorithm is regarding ellipsotopes as a combination of some spectrahedral shadows under the translation, linear map and intersections. Specifically, for arbitrary $\mathcal{E}_p(c, G, A, b, \mathcal{J}) = \{x \in \mathbb{R}^n : x = c + G\xi, \|\xi\|_p \leq 1, \forall J \in \mathcal{J}, Ax = b\}$ with $\mathcal{J} = \{J_1, J_2, \dots, J_{|\mathcal{J}|}\} \subset \mathbb{P}(\mathbb{N})$, we have

$$\mathcal{E}_p(c, G, A, b, \mathcal{J}) = c + G \circ (\mathcal{P}(A, b) \cap \mathcal{P}(A, -b) \cap \mathcal{B}_p^\times(\mathcal{J})),$$

where $\mathcal{B}_p^\times(\mathcal{J}) = \{x \in \mathbb{R}^n : \|\xi\|_p \leq 1, \forall J \in \mathcal{J}\}$. In [12], $\mathcal{B}_p^\times(\mathcal{J})$ is referred to as a *ball product*, which is equivalently written as

$$\mathcal{B}_p^\times(\mathcal{J}) = \mathcal{B}_p^{|J_1|} \times \mathcal{B}_p^{|J_2|} \times \dots \times \mathcal{B}_p^{|J_{|\mathcal{J}|}|}. \quad (27)$$

It has been shown in [37, (3.3.37)] that any \mathcal{B}_p^n with rational p can be formulated as conic quadratic-representable sets, and such sets can be further formulated as spectrahedral shadows [37, (4.2.1)]. Since all required set operations have been given in Section III-A, it yields Algorithm 1.

IV. COMPLEXITY REDUCTION STRATEGY

For spectrahedral shadows, the growth of size and lifted dimension is a realistic issue when iteratively implementing set operations like the Minkowski sum. This issue commonly exists in SE, RA and FD [13], [15], resulting in the increase of time and space overhead for subsequent set operations. Thus, reducing the complexity of spectrahedral shadows is necessary for many set-based applications.

Algorithm 1: Conversion from Ellipsotopes**Input:** $\mathcal{E}_p(c, G, A, b, \mathcal{J})$ with $\mathcal{J} = \{J_1, J_2, \dots, J_{|\mathcal{J}|}\}$;**Output:** the spectrahedral shadow $\langle A, \{A_i\}_{i=1}^n, \{B_i\}_{i=1}^m \rangle$;

- 1: Formulate $\mathcal{B}_p^{J_1}, \mathcal{B}_p^{J_2}, \dots, \mathcal{B}_p^{J_{|\mathcal{J}|}}$ as spectrahedral shadows using (3.3.37) and (4.2.1) in [37];
- 2: Compute $\mathcal{B}_p^\times(\mathcal{J})$ according to (27) and Proposition 5;
- 3: Formulate $\mathcal{P}(A, b)$ and $\mathcal{P}(A, -b)$ as spectrahedral shadows using Lemma 7;
- 4: Compute $\mathcal{S}_e = \mathcal{P}(A, b) \cap \mathcal{P}(A, -b) \cap \mathcal{B}_p^\times(\mathcal{J})$ using Lemma 4;
- 5: Compute $\langle A, \{A_i\}_{i=1}^n, \{B_i\}_{i=1}^m \rangle = c + G \circ \mathcal{S}_e$ using Propositions 1 and 2;

In this section, we first propose a method called *local low-rank approximation* to compute a lower size spectrahedron as the outer approximation of a given spectrahedron. Then we discuss how to reduce the size and eliminate the lifted dimensions for general spectrahedral shadows. Finally, we provide strategies to accelerate the above complexity-reducing process in practice by utilizing the sparsity of spectrahedral shadows.

A. Order Reduction of Spectrahedrons

For brevity, we use $\Lambda(x) = \Lambda + \sum_{i=1}^n x_i A_i$ and $\Lambda(x, y) = \Lambda + \sum_{i=1}^n x_i A_i + \sum_{i=1}^m y_i B_i$ to denote the linear matrix pencils in this section. Assume that $\mathcal{S}_g = \{x \in \mathbb{R}^n : \Lambda(x) \succeq 0\}$ is a full-dimensional bounded spectrahedron to be reduced size with size s_g and there are N different points x^1, x^2, \dots, x^N on the boundary of \mathcal{S}_g (i.e., $x_i \in \text{bd}(\mathcal{S}_g)$). The idea of the local low-rank approximation is to produce a reduced-size spectrahedron $\mathcal{S}_r = \mathcal{S}_r^1 \cap \mathcal{S}_r^2 \cap \dots \cap \mathcal{S}_r^N$ with the size s_r such that:

- 1) $\mathcal{S}_g \subseteq \mathcal{S}_r^i, \forall 1 \leq i \leq N$;
- 2) Each \mathcal{S}_r^i locally approximates \mathcal{S}_g at the point x^i .
Namely, \mathcal{S}_g is internally tangent to \mathcal{S}_r^i at x^i .

Fig. 4 gives an example to illustrate the above process.

Next, we elaborate on the proposed method. Consider that there is a matrix $P^i \in \mathbb{R}^{s_g \times s_r^i}$. Each \mathcal{S}_r^i is computed based on the following implication:

$$\Lambda(x) \succeq 0 \Rightarrow (P^i)^T \Lambda(x) P^i \succeq 0. \quad (28)$$

Let $\mathcal{S}_r^i = \{x \in \mathbb{R}^n : (P^i)^T \Lambda(x) P^i \succeq 0\}$. Then we have $\mathcal{S}_g \subseteq \mathcal{S}_r^i$ for arbitrary P^i .

Then we show how to choose the proper P^i such that \mathcal{S}_r^i locally approximates \mathcal{S}_g at x^i . Specifically, assume that the SVD of $\Lambda(x^i)$ is $\Lambda(x^i) = U^i D^i (U^i)^T$, where D^i is a diagonal matrix such that $D_{[j,j]}^i$ ($1 \leq j \leq s_g$) is the j -th largest singular value of $\Lambda(x^i)$. Then P^i is given by

$$P^i = [U_{[*], s_g - s_r + 1}^i, U_{[*], s_g - s_r + 2}^i, \dots, U_{[*], s_g}^i]. \quad (29)$$

Since the necessary and sufficient condition for $x \in \text{bd}(\mathcal{S}_g)$ is $\det(\Lambda(x)) = 0$ [40, Theorem 3.2.3], we can prove that $x^i \in \text{bd}(\mathcal{S}_g)$ implies $x^i \in \text{bd}(\mathcal{S}_r^i)$ with such a choice of P^i . Due to $\mathcal{S}_g \subseteq \mathcal{S}_r^i$ and $x^i \in \text{bd}(\mathcal{S}_r^i) \cap \text{bd}(\mathcal{S}_g)$, \mathcal{S}_g is internally tangent to \mathcal{S}_r^i at x^i . Moreover, it is clear that:

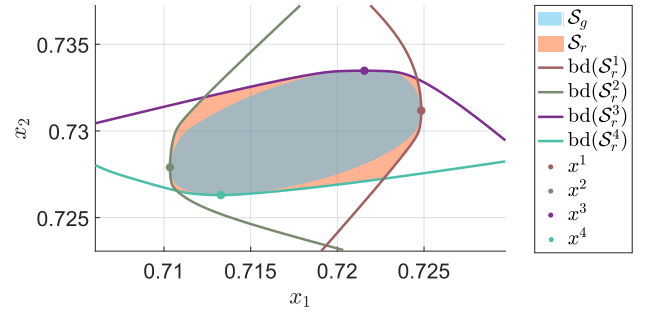


Fig. 4. Example of local low rank approximation. \mathcal{S}_g is a spectrahedron to be reduced size ($s_g = 50$). $\mathcal{S}_r = \mathcal{S}_r^1 \cap \mathcal{S}_r^2 \cap \mathcal{S}_r^3 \cap \mathcal{S}_r^4$ is the reduced-size spectrahedron ($s_r = 40$). $\text{bd}(\mathcal{S}_r^i)$ ($1 \leq i \leq 4$) is the part of the boundary of \mathcal{S}_r^i that locally approximates $\text{bd}(\mathcal{S}_g)$ at x^i .

- 1) When $\text{rank}(P^i) \geq s_r$, \mathcal{S}_r^i is exactly \mathcal{S}_g ;
- 2) When $\text{rank}(P^i) = 1$, \mathcal{S}_r^i is a half-space and $\text{bd}(\mathcal{S}_r^i)$ is the hyperplane tangent to \mathcal{S}_g at x^i .

For $1 < \text{rank}(P^i) < s_r$, our numerical experiments show that with the increase of $\text{rank}(P^i)$, the approximation of \mathcal{S}_r^i to \mathcal{S}_g becomes more accurate.

The remaining issue is the choice of boundary points x^1, x^2, \dots, x^N . After experimenting with various strategies, an efficient heuristic is found to be choosing $N = 2n$ and

$$x^i = \begin{cases} \arg \max_{x \in \mathcal{S}_g} x_i, & 1 \leq i \leq n \\ \arg \min_{x \in \mathcal{S}_g} x_{i-n}, & n+1 \leq i \leq 2n \end{cases} \quad (30)$$

if the shape of \mathcal{S}_g is approximately isotropic (e.g., approximates a unit ball or a hypercube). In practice, since \mathcal{S}_g does not always approximate to an isotropic set (e.g., the shape of \mathcal{S}_g may be long and narrow), we can find a nonsingular transformation matrix $T^* \in \mathbb{R}^{n \times n}$ such that $\mathcal{S}_g' = T^* \circ \mathcal{S}_g$ is an isotropic set (see Appendix I for the details). By applying the above process, a reduced-size spectrahedron \mathcal{S}_r' is computed for \mathcal{S}_g' . Thus, $\mathcal{S}_r = \mathcal{S}_r' \circ T^*$ is the reduced-size spectrahedron for \mathcal{S}_g .

By properly choosing s_r^i such that $s_r = \sum_{i=1}^N s_r^i \leq s_g$, the above process leads to a reduced-size spectrahedron \mathcal{S}_r .

Example 2: To assess the effectiveness, Fig. 5 shows the box plot for the volume ratio² of \mathcal{S}_g and \mathcal{S}_r over 4 groups of examples. In each group, we randomly generate 100 n -dimensional \mathcal{S}_g , and compute \mathcal{S}_r with the size s_r by the proposed method, where s_r^i ($1 \leq i \leq 2n$) is chosen as $s_r^i = \frac{s_r}{2n}$. In Fig. 5, it is observed that the reduced-size spectrahedron \mathcal{S}_r efficiently approximates \mathcal{S}_g , and the approximation becomes more accurate with the decrease in the size to be reduced.

B. Polyhedral Approximation of Spectrahedral Shadows

It is tricky to find a general spectrahedral shadow with smaller size and lifted dimensions to outer approximate the given spectrahedral shadow, as the analytical volume metric for spectrahedral shadows remains an open problem and the containment problem for spectrahedral shadows is co-NP-hard [41]. However, polyhedral approximation of spectrahedral

²In this paper, the volume computation for spectrahedral shadows are computed by high precision boundary sampling, as there is currently no analytical expression for computing the volume of spectrahedral shadows.

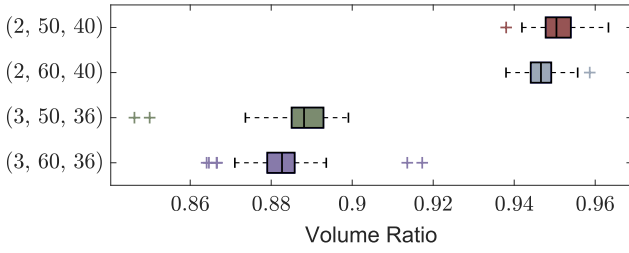


Fig. 5. The box plot for the volume ratio ΔV of \mathcal{S}_g and \mathcal{S}_r . Each row label (n, s_g, s_r) corresponds to a group of results for 100 random simulations, where the spectrahedron $\mathcal{S}_g \subset \mathbb{R}^n$ with the size s_g is outer approximated by the spectrahedron $\mathcal{S}_r \subset \mathbb{R}^n$ with the size s_r .

shadows is feasible, and polyhedrons are readily written as spectrahedrons (see Lemma 7). Thus, it is practical to use polyhedral approximation to reduce the size and eliminate the lifted dimensions for spectrahedral shadows, on condition that the accuracy and time efficiency meet expectations.

Consider a full-dimensional bounded spectrahedral shadow $\mathcal{S}_g = \{x \in \mathbb{R}^n : \exists y \in \mathbb{R}^m, \Lambda(x, y) \succeq 0\}$. For an arbitrary direction $a^i \in \mathbb{R}^n$, it is observed that $\mathcal{H}^i = \{x \in \mathbb{R}^n : (a^i)^T x \leq b^i\}$ is a half-space externally tangent to \mathcal{S}_g when $b^i = \max_{x \in \mathcal{S}_g} (a^i)^T x$. Thus, by choosing s_r directions $a^1, a^2, \dots, a^{s_r} \in \mathbb{R}^n$, a polyhedron $\mathcal{P}(A^r, b^r)$ externally tangent to \mathcal{S}_g is computed by solving the SDP problem

$$(\bar{x}^1, \dots, \bar{x}^{s_r}, \bar{y}^1, \dots, \bar{y}^{s_r}) = \arg \max_{x^1, \dots, x^{s_r}, y^1, \dots, y^{s_r}} \sum_{i=1}^{s_r} (a^i)^T x^i \quad (31)$$

$$\text{s.t.}, \Lambda(x^i, y^i) \succeq 0, \forall 1 \leq i \leq s_r,$$

where $x^i \in \mathbb{R}^n$, $y^i \in \mathbb{R}^m$, $(A^r)^T = [a^1, a^2, \dots, a^{s_r}]$ and $b^r = [(a^1)^T \bar{x}^1, (a^2)^T \bar{x}^2, \dots, (a^{s_r})^T \bar{x}^{s_r}]^T$. By Lemma 7, $\mathcal{P}(A^r, b^r)$ is further written as a spectrahedron with the size s_r . To make the polyhedral approximation for \mathcal{S}_g in different directions as uniform as possible, we apply the geometric procedure in [42] to generate the direction vectors a^1, a^2, \dots, a^{s_r} , which ensures $a^1, a^2, \dots, a^{s_r} \in \mathbb{R}^n$ with arbitrary n and s_r are unit vectors almost uniformly distributed on an n -dimensional hyper-sphere.

The above is a brief introduction to polyhedral approximation for \mathcal{S}_g . In Section IV-C, we discuss how to improve the time efficiency in practice. Moreover, the effectiveness will be demonstrated by numerical examples in Section V.

C. Acceleration using Sparsity

When applied to SE, RA, and FD, spectrahedral shadows with large size and lifted dimensions typically result from the propagation of some basic spectrahedral shadows through set operations in Section III-A, which endows these sets with sparse structures. Specifically, such spectrahedral shadows $\mathcal{S}_g = \{x \in \mathbb{R}^n : \exists y \in \mathbb{R}^m, \Lambda(x, y) \succeq 0\}$ with size s_g can be decomposed into

$$\Lambda(x, y) = \begin{bmatrix} \Lambda^{(1)}(x, y) & \mathbf{0} & \dots & \mathbf{0} \\ \mathbf{0} & \Lambda^{(2)}(x, y) & \dots & \mathbf{0} \\ \vdots & \vdots & \ddots & \vdots \\ \mathbf{0} & \mathbf{0} & \dots & \Lambda^{(l)}(x, y) \end{bmatrix} \quad (32)$$

where $\Lambda^{(i)}(x, y) = \Lambda^{(i)} + \sum_{j=1}^n x_j A_j^{(i)} + \sum_{j=1}^m y_j B_j^{(i)}$, $\Lambda^{(i)}, A_j^{(i)}, B_j^{(i)} \in \mathbb{S}^{s_g^{(i)}}$, and the inequality $s_g^2 \gg n + m$ typically holds.

In practice, the efficiency of implementing the set validations in Section III-B and the complexity reduction strategies in Section IV is dominated by solving certain SDP problems, e.g., (22), (30) and (31). In the following parts, we will take (31) as an example to show that through utilizing the structure of \mathcal{S}_g , these SDP problems can be solved far more efficiently.

When directly solving (31), the state-of-the-art interior point method for SDP [28] and SDP solvers (e.g., Mosek [43]) treat the constraints of (31) as

$$X^{(i)} = \Lambda(x^i, y^i), X^{(i)} \succeq 0, \forall 1 \leq i \leq s_r \quad (33)$$

by introducing SDP variables $X^{(1)}, X^{(2)}, \dots, X^{(s_r)} \in \mathbb{S}^{s_g}$. This means that such a problem has $\frac{s_r s_g (s_g + 1)}{2}$ equality constraints, $s_r(m + n)$ scalarized variables, and $\frac{s_r s_g (s_g + 1)}{2}$ scalar SDP variables. On the other hand, by using the decomposition (32), the constraints in (31) can be written as

$$\Lambda^{(i)}(x^j, y^j) \succeq 0, \forall 1 \leq i \leq l, 1 \leq j \leq s_r. \quad (34)$$

With (34), we further consider the dual problem of (31), i.e.,

$$(\bar{Z}^{(1,1)}, \dots, \bar{Z}^{(s_r, l)}) = \arg \min_{Z^{(i,j)}} \sum_{i=1}^{s_r} \sum_{j=1}^l \text{tr}(\Lambda^{(j)} Z^{(i,j)})$$

$$\text{s.t.}, Z^{(i,j)} \succeq 0, \forall 1 \leq i \leq s_r, 1 \leq j \leq l,$$

$$a_k^i + \sum_{j=1}^l \text{tr}(A_k^{(j)} Z^{(i,j)}) = 0, \forall 1 \leq i \leq s_r, 1 \leq k \leq n,$$

$$\sum_{j=1}^l \text{tr}(B_t^{(j)} Z^{(i,j)}) = 0, \forall 1 \leq i \leq s_r, 1 \leq t \leq m, \quad (35)$$

where the multiplier $Z^{(i,j)} \in \mathbb{S}^{s_g^{(j)}}$. Note that since \mathcal{S}_g is full-dimensional, there exists a congruence transformation such that the inequalities (34) are strictly feasible [44, Corollary 5]. By Slater condition, the strong duality holds for (31) and (35), and hence $(a^i)^T \bar{x}^i = \sum_{j=1}^l \text{tr}(\Lambda^{(j)} \bar{Z}^{(i,j)})$.

The problem (35) has $s_r(m + n)$ equality constraints and $\sum_{i=1}^l \frac{s_r s_g^{(i)} (s_g^{(i)} + 1)}{2}$ scalarized SDP variables. Due to $s_g^2 \gg n + m$ and $s_g = \sum_{i=1}^l s_g^{(i)}$, both the equality constraints and scalarized SDP variables have been significantly reduced compared with the original problem (31). We give the following example to illustrate the improvement of efficiency.

Example 3: Consider the following dynamics commonly seen in SE, RA and FD

$$\mathcal{X}_{k+1} = \mathcal{A}_k \circ \mathcal{X}_k \oplus \mathcal{B}_k \circ \mathcal{U}_k, \quad (36)$$

where $\mathcal{A}_k, \mathcal{B}_k \in \mathbb{R}^{n \times n}$ and $\mathcal{X}_k, \mathcal{U}_k \subset \mathbb{R}^n$. Assume that \mathcal{X}_0 is an H-polyhedron with n_h hyperplanes and each \mathcal{U}_k is an ellipsoid. By representing \mathcal{X}_0 and \mathcal{U}_k as a spectrahedral shadow, \mathcal{X}_k will be a spectrahedral shadow with large size and lifted dimensions if k is large enough. For instance, if $n = 3$, $n_h = 5$, the size and lifted dimension of \mathcal{X}_{30} are $s_g = 126$ and $m_g = 90$. If we compute a size-reduced spectrahedron $\hat{\mathcal{X}}_{30}$ with the size $s_r = 20$ using the polyhedral approximation

in Section IV-B, the problem (35) will have $n_{ec} = 157500$ equality constraints, $n_{sv} = 1860$ scalar variables and $n_{sdp} = 157500$ scalarized SDP variables. As a comparison, \mathcal{X}_{30} can be decomposed into the form of (32) with $l = 36$, and the problem (31) will only have $n_{ec} = 1860$ equality constraints and $n_{sdp} = 6100$ scalarized SDP variables. Moreover, Table I shows the scale and solving time for the problems (31) and (35) with different $n + m_g$, s_g and s_r , where solving time t_a is averaged over 100 runs³. From Table I, it is observed that the polyhedral approximation in Section IV-B is remarkably accelerated by utilizing the sparsity of \mathcal{X}_k . With fixed s_r , the time consumption to solve the problem (35) increases linearly in terms of $n + m_g$ and s_g . Moreover, the problem (31) becomes unsolvable when $n + m_g = 150$ and $s_g = 210$ due to out of memory, but the problem (35) still can be efficiently solved.

TABLE I
PROBLEM SCALE AND AVERAGE SOLVING TIME.

$n + m_g$ ¹	s_g	s_r	Problem (31)			Problem (35)		
			n_{ec}	n_{sdp}	t_a [s]	n_{ec}	n_{sdp}	t_a [s]
50	70	10	24850	24850	5.08	500	1600	0.05
		15	37275	37275	7.44	750	2400	0.07
100	140	10	98700	98700	117	1000	3200	0.08
		15	148050	148050	165	1500	4800	0.11
150	210	10	221550	221550	—	1500	4800	0.12
		20	443100	443100	—	3000	9600	0.23

¹ Note that the complexity of the problems (31) and (35) is proportional to $n + m_g$, instead of the single n or m_g .

V. STATE ESTIMATION WITH MIXED POLYTOPIC AND QUADRATIC UNCERTAINTIES

This section considers set-membership estimation [9] to demonstrate set operations of spectrahedral shadows and their space overhead and efficiency advantages for high-dimensional systems. Specifically, consider the linear system

$$x_{k+1} = \mathcal{A}x_k + \mathcal{B}u_k + \mathcal{L}\omega_k, \quad y_k = \mathcal{C}x_k + \mathcal{F}v_k \quad (37)$$

with state $x_k \in \mathbb{R}^{n_x}$, input $u_k \in \mathbb{R}^{n_u}$, output $y_k \in \mathbb{R}^{n_y}$, disturbance $\omega_k \in \mathbb{R}^{n_\omega}$ and measurement noise $v_k \in \mathbb{R}^{n_v}$. This example considers the case that x_0 and ω_k are bounded by component, and the energy of v_k is limited. Specifically, $x_0 \in \mathcal{X}_0$, $\omega_k \in \mathcal{W}$ and $v_k \in \mathcal{V}$, where \mathcal{V} is an ellipsoid, and both \mathcal{X}_0 and \mathcal{W} are hypercubes.

Set-membership estimation is a classical set-based state estimator proven to be optimal for linear systems [2], which can produce the tightest state estimation set X_k containing x_k if all computation is exact. For set-membership estimation, \mathcal{X}_k is obtained from $\mathcal{X}_k = \tilde{\mathcal{X}}_k \cap \tilde{\mathcal{X}}_k$, where

$$\tilde{\mathcal{X}}_{k+1} = (\mathcal{A} \circ \mathcal{X}_k + \mathcal{B}u_k) \oplus \mathcal{L} \circ \mathcal{W}, \quad (38a)$$

$$\tilde{\mathcal{X}}_k = (y_k + (-\mathcal{F} \circ \mathcal{V})) \circ \mathcal{C} \quad (38b)$$

³ All numerical examples in this paper are carried out in MATLAB 2024b on an AMD R9 7940HX processor with 2×16 GB memory, and the formulated optimization problems are solved by Mosek 10.2.8 [43].

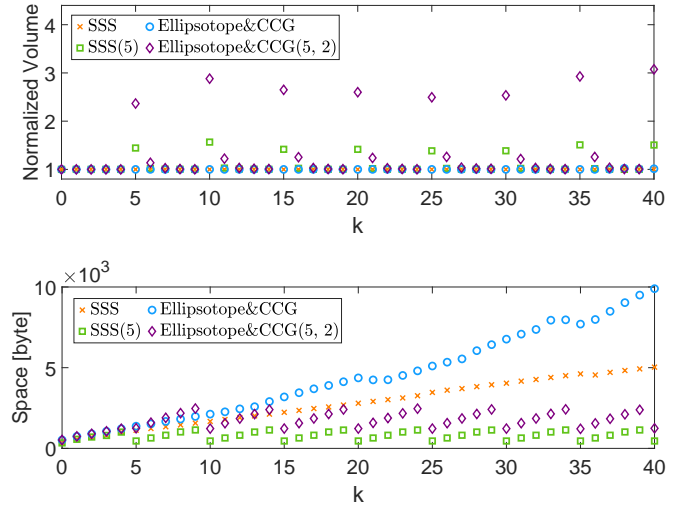


Fig. 6. The average volume and space overhead of \mathcal{X}_k using SSS, SSS(5), *Ellipsotope&CCG* and *Ellipsotope&CCG(5, 2)* on random 2-dimensional systems.

According to (38b), the consistent state set $\tilde{\mathcal{X}}_k$ will be an unbounded set if the number of system sensors is fewer than system states (i.e., $\text{rank}(\mathcal{C}) < n_x$). By representing X_0 , \mathcal{W} and \mathcal{V} as spectrahedral shadows, we can compute the exact \mathcal{X}_k using the set operations in Section III-A.

For comparison, we also compute \mathcal{X}_k using ellipsotopes and CCGs (the representation and implementation of ellipsotopes and CCGs are consistent for this task) via the open source code [12] and the state-of-the-art complexity reduction strategies of CCGs [15, Algorithms 1 and 2]. Note that we do not evaluate set representations like zonotopes and ellipsoids, since the uncertainties considered in this example are mixed polytopic and quadratic, and hence these set representations require outer approximation to represent \mathcal{W} or \mathcal{V} , resulting in extra loss of accuracy. For this case, the example in [12, Section V-C] has shown that ellipsotopes and CCGs maintain comparable speed but provide a tighter result.

We first evaluate \mathcal{X}_k for $0 \leq k \leq 40$ on 100 random linear systems (37) with the dimension $d = n_x = n_u = n_y = n_\omega = n_v = 2$. As shown in Fig.6, SSS denotes the results using spectrahedral shadows without reducing complexity, *Ellipsotope&CCG* denotes the results using ellipsotopes (or equivalently, CCGs) without reducing complexity, $\text{SSS}(s_r/n_x)$ denotes the results using spectrahedral shadows and applying the complexity reduction strategy in Section IV-B per 5 steps that approximates \mathcal{X}_k as an n_x -dimensional spectrahedron with size s_r , and *Ellipsotope&CCG*($n_g/n_x, n_c/n_x$) denotes the results using ellipsotopes and applying the complexity reduction strategy in [15, Algorithms 1 and 2] per 5 steps that approximates \mathcal{X}_k as an n_x -dimensional ellipsotope with n_g generators and n_c constraints. The parameter d_i in [15, Algorithm 1] is set as $\frac{1}{n_p}$ according to the recommendation in [15]. The methods SSS and $\text{SSS}(s_r/n_x)$ use sparse forms (see Remark 1). Thus, for a fair comparison, all parametric matrices of ellipsotopes and CCGs that possibly have a large number of zero elements (e.g., constraints and generator matrices) are compressed into sparse matrices when calculating the space

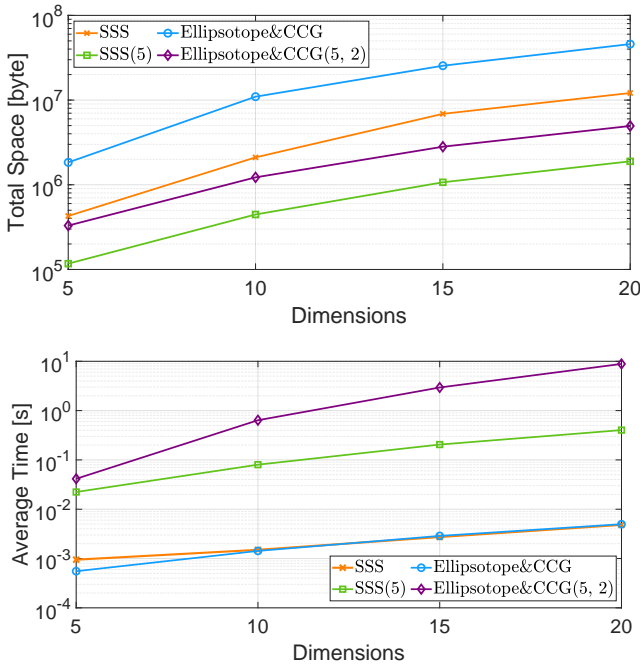


Fig. 7. The total space overhead of X_k from $k = 0$ to $k = 40$ and the average time consumption in each step on high dimensional systems.

overhead. The volume results are normalized based on SSS, as X_k calculated by SSS is the *exact* state estimation set.

Apart from results in Fig.6, the average time consumption in each step is 0.37 ms (SSS), 0.31 ms (*Ellipsotope&CCG*), 4.61 ms (SSS(5)) and 2.17 ms (*Ellipsotope&CCG*(5, 2)). From these results, it can be seen that the space overhead of set representations will increase constantly if no complexity reduction strategy is implemented, but reducing the complexity of set representations results in a loss of accuracy and extra time overhead. Compared with ellipsotopes and CCGs, spectrahedral shadows have smaller space overhead, especially for high-order sets. The time consumption of SSS and *Ellipsotope&CCG* is comparable, but the time consumption of SSS(5) is about 2.1 times that of *Ellipsotope&CCG*(5, 2) for 2-dimensional cases, and the reason will be discussed later. In Fig. 6, the volume results of SSS(5) illustrate the effectiveness of the complexity reduction strategy in Section IV-B.

Furthermore, we evaluate X_k for $0 \leq k \leq 40$ with the dimension $d = n_x = n_u = n_y = n_\omega = n_v = \{5, 10, 15, 20\}$. The results are averaged over 100 random systems (37) and shown in Fig. 7. Consistent with research like [27], the volume results were not considered for this high dimensional example, since we aim at illustrating the space overhead and efficiency advantages of spectrahedral shadows, and calculating the exact volume of high-dimensional spectrahedral shadows is impractical due to its NP-hardness².

From Fig. 7, it is observed that the space overhead of spectrahedral shadows is remarkably lower than that of ellipsotopes and CCGs, regardless of whether the complexity reduction strategy is adopted. Although the computational complexity of operations like linear mapping and Minkowski sum of spectrahedral shadows is higher than that of ellipsotopes and CCGs (see Section III-A and [12, Section IV-B]), the time

consumption of SSS and *Ellipsotope&CCG* is still comparable on high dimensional cases. This is because the practical time efficiency is determined by both the computational complexity and the input scale, and the time consumption caused by the high computational complexity of spectrahedral shadows is offset by the time savings brought by their low space overhead. Different from the 2-dimensional case, the time consumption of SSS(5) is lower than that of *Ellipsotope&CCG*(5, 2) for high dimensional cases, and the difference becomes more noticeable with the increase in dimensions. This is because the time consumption of *Ellipsotope&CCG*(5, 2) mainly results from the constraint reduction strategy [15, Algorithm 2] that has $\mathcal{O}(n_c^r n_c^2 n_g^2)$ complexity, where n_c^r , n_c and n_g are the number of constraints to be reduced, the number of constraints, and the number of generators, respectively. However, with the sparse acceleration strategy in Section IV-C, the time consumption of the polyhedral approximation in Section IV-B increases linearly in terms of the dimension, the lifted dimension and the size of spectrahedral shadows, just as demonstrated in Example 3. In summary, the above results demonstrate the space overhead and efficiency advantages of spectrahedral shadows for modeling uncertainties with complex form (e.g., mixed polytopic and ellipsoidal), especially for high dimensional systems.

VI. REACHABLE SET OF MINKOWSKI-FIREY L_p SUMS OF ELLIPSOIDS

This section uses the example of reachable analysis taken from [3] to demonstrate the Minkowski-Firey L_p sum of spectrahedral shadows. Specifically, consider the linear system with the dynamics $x_{k+1} = \mathcal{A}x_k + \mathcal{B}u_k$, where the initial state $x_0 \in \mathcal{X}_0$ and input $u_k \in \mathcal{U}_k$. We want to compute a reachable set X_k such that $x_k \in X_k$ holds for arbitrary x_0 and u_k . To make the description of uncertainty more flexible, the sets \mathcal{X}_0 and \mathcal{U}_k in [3] are modeled as the Minkowski-Firey L_p sums of ellipsoids, i.e.,

$$\mathcal{X}_0 = \mathcal{E}(\bar{x}_0, Q_1^0) +_{p_1} \dots +_{p_1} \mathcal{E}(\bar{x}_0, Q_{m_x}^0) \quad (39a)$$

$$\mathcal{U}_k = \mathcal{E}(\bar{u}_k, U_1^k) +_{p_2} \dots +_{p_2} \mathcal{E}(\bar{u}_k, U_{m_u}^k), \quad (39b)$$

where $p_1, p_2 \geq 1$, $Q_i^0 \in \mathbb{S}^{n_x}$ for $1 \leq i \leq m_x$, $U_j^k \in \mathbb{S}^{n_u}$ for $1 \leq j \leq m_u$, and $\bar{x}_0 \in \mathbb{R}^{n_x}$ and $\bar{u}_k \in \mathbb{R}^{n_u}$ are the nominal initial state and control, respectively.

In this example, we take $p_1 = 3$ and $p_2 = 1.5$ to compute the reachable set X_k using spectrahedral shadows. For this task, Algorithms 1 and 2 in [3] are the only two available methods in the literature to the best of our knowledge. In this section, both methods are used for comparison and marked as MTOE and MVOE, respectively. The error tolerance of [3, Algorithm 2] is set to 10^{-5} . The method to compute X_k , the initial conditions (e.g., m_x and m_u) and the system parameters are all consistent with the example in [3, Section VI-B]. The results from $k = 1, 2, \dots, 10$ are shown in Fig. 8 and Table. II. It is observed from Fig. 8 and Table. II that spectrahedral shadows maintain comparable computational speed but provide much tighter reachable sets compared with MTOE and MVOE. This is because the reachable sets computed by spectrahedral shadows are *exact*, rather than being the outer-approximated ellipsoids like previous methods.

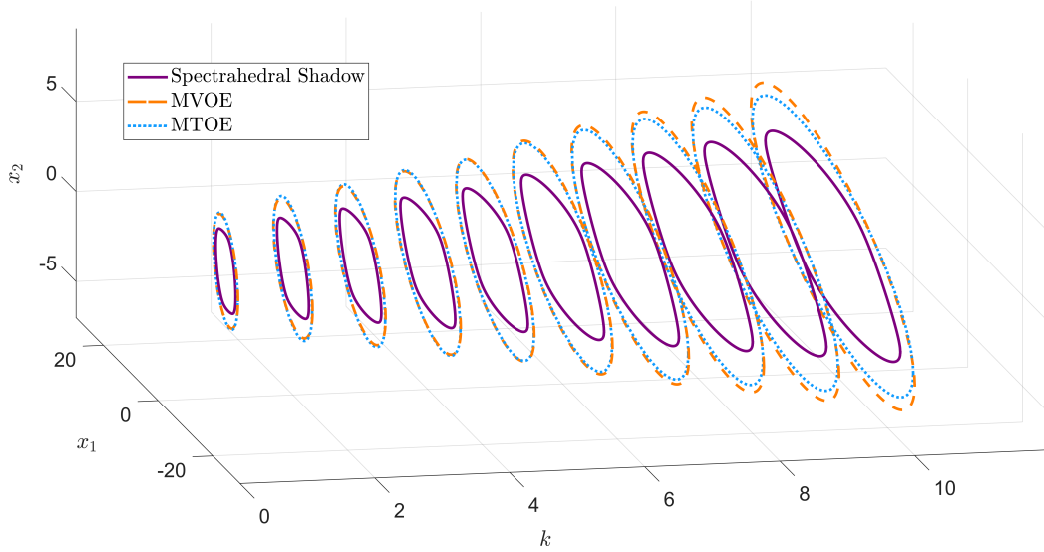


Fig. 8. The boundaries of reachable sets calculated by spectrahedral shadows, MVOE and MTOE for the system given in [3, Section VI-B].

TABLE II
THE VOLUME OF REACHABLE SETS AND THE AVERAGE TIME CONSUMPTION IN EACH TIME INSTANT.

Methods	Vol(X_k)										Average time [s]
	$k = 1$	$k = 2$	$k = 3$	$k = 4$	$k = 5$	$k = 6$	$k = 7$	$k = 8$	$k = 9$	$k = 10$	
Spectrahedral shadow	24.021	41.552	56.444	78.738	96.420	133.429	165.061	192.471	222.664	257.184	9.383×10^{-4}
MTOE [3, Algorithm 1]	38.933	70.919	95.440	135.109	164.383	228.112	279.374	320.440	365.306	416.895	5.612×10^{-4}
MVOE [3, Algorithm 2]	38.984	70.202	95.239	135.565	167.269	234.810	291.711	338.986	391.206	451.066	6.968×10^{-4}

VII. CONCLUSION

The paper investigates the necessary techniques to apply spectrahedral shadows on tasks such as reachability analysis and set-based state estimation. Spectrahedral shadows can flexibly model uncertainties in practical tasks, such as those in mixed polytopic and ellipsoidal form, or even convex polynomial form. Compared with the advanced set representations like ellipsotopes and constrained convex generators, spectrahedral shadows support more set operations without approximation, and have lower space overhead due to their conciseness and sparse structure. Although the theoretical complexity of common set operations like linear map and Minkowski sum for spectrahedral shadows is higher, the numerical example demonstrates that the practical time consumption of these operations is comparable with ellipsotopes because of the time savings resulting from the lower space overhead. Future work will focus on the flexible complexity reduction methods for spectrahedral shadows to achieve less conservative results.

ACKNOWLEDGMENT

The authors would like to thank Prof. Feng Xu for the useful discussion on the topic of set representation, and Prof. Graziano Chesi for inspiring the authors to apply LMIs in modeling uncertainties.

APPENDIX I THE COMPUTATION OF T^*

Consider a parameterized parallelotope $\mathcal{P}_z = \mathcal{Z}(c, T^{-1})$ (i.e., an n -dimensional zonotope with n generators) with $T \succ 0$. Our aim is to find an optimal (c^*, T^*) such that $\mathcal{P}_z^* = \mathcal{Z}(c^*, (T^*)^{-1})$ is the minimum volume parallelotope containing $\mathcal{S}_g = \{x \in \mathbb{R}^n : A + \sum_{i=1}^n x_i A_i \succeq 0\}$. With such T^* , $T^* \circ \mathcal{P}_z^* = \mathcal{Z}(T^* c^*, I)$ is an n -dimensional hypercube. Due to the affine invariance of minimum volume enclosing sets (see [45, Section 8.4.3]), the hypercube $T^* \circ \mathcal{P}_z^*$ is the minimum volume parallelotope containing $\mathcal{S}'_g = T^* \circ \mathcal{S}_g$. Hence, \mathcal{S}'_g approximates an isotropic set.

Then we elaborate on the computation of T^* . According to Proposition 11, $\mathcal{P}_z = \mathcal{Z}(c, T^{-1})$ can be rewritten as the spectrahedron $\langle A^z, \{A_i^z\}_{i=1}^n \rangle$ with

$$\begin{aligned} A^z &= I_{2n} - \text{diag}(c'_1, c'_2, \dots, c'_n, -c'_1, -c'_2, \dots, -c'_n), \\ A_i^z &= \text{diag}(T_{[1,i]}, T_{[2,i]}, \dots, T_{[n,i]}, -T_{[1,i]}, -T_{[2,i]}, \dots, \\ &\quad -T_{[n,i]}), \forall 1 \leq i \leq n, \end{aligned}$$

where $c' = Tc$. It is observed that \mathcal{P}_z is also a polytope. According to [41, Theorem 4.8], [41, Lemma 4.5] and [46, Proposition 4.2], $\mathcal{S}_g \subset \mathcal{P}_z$ iff there exist $O^1, O^2, \dots, O^{2n} \in \mathbb{S}^{s_g}$

such that $O^1, O^2, \dots, O^{2n} \succeq 0$ and

$$\begin{aligned} T_{[i,j]} &= \sum_{k=1}^{s_g} \sum_{l=1}^{s_g} A_{j,[k,l]} O_{[k,l]}^i, \quad 1 + c'_i = \sum_{k=1}^{s_g} \sum_{l=1}^{s_g} A_{[k,l]} O_{[k,l]}^i, \\ -T_{[i,j]} &= \sum_{k=1}^{s_g} \sum_{l=1}^{s_g} A_{j,[k,l]} O_{[k,l]}^{i+n}, \quad 1 - c'_i = \sum_{k=1}^{s_g} \sum_{l=1}^{s_g} A_{[k,l]} O_{[k,l]}^{i+n}, \\ &\quad \forall i = 1, \dots, n, \quad j = 1, \dots, n \end{aligned} \quad (40)$$

where $A_{j,[k,l]}$ denotes the element in k -th row and l -th column of A_j . Since the volume of \mathcal{P}_z is $\text{vol}(\mathcal{P}_z) = 2^n \det(T^{-1})$ [9], T^* can be obtained by solving the SDP problem

$$\min_{T, c', O^1, \dots, O^{2n}} \log \det T^{-1} \quad (41a)$$

$$\text{s.t.}, \quad O^1 \succeq 0, \dots, O^{2n} \succeq 0, \quad (40). \quad (41b)$$

REFERENCES

- [1] F. Schweppe, "Recursive state estimation: Unknown but bounded errors and system inputs," *IEEE Transactions on Automatic Control*, vol. 13, no. 1, pp. 22–28, 2003.
- [2] Y. Cong, X. Wang, and X. Zhou, "Rethinking the mathematical framework and optimality of set-membership filtering," *IEEE Transactions on Automatic Control*, vol. 67, no. 5, pp. 2544–2551, 2021.
- [3] A. Halder, "Smallest ellipsoid containing p -sum of ellipsoids with application to reachability analysis," *IEEE Transactions on Automatic Control*, vol. 66, no. 6, pp. 2512–2525, 2020.
- [4] M. Althoff and J. M. Dolan, "Online verification of automated road vehicles using reachability analysis," *IEEE Transactions on Robotics*, vol. 30, no. 4, pp. 903–918, 2014.
- [5] F. Xu, J. Tan, Y. Wang, X. Wang, B. Liang, and B. Yuan, "Robust fault detection and set-theoretic UIO for discrete-time LPV systems with state and output equations scheduled by inexact scheduling variables," *IEEE Transactions on Automatic Control*, vol. 64, no. 12, pp. 4982–4997, 2019.
- [6] J. K. Scott, D. M. Raimondo, G. R. Marseglia, and R. D. Braatz, "Constrained zonotopes: A new tool for set-based estimation and fault detection," *Automatica*, vol. 69, pp. 126–136, 2016.
- [7] M. Althoff, "Reachability analysis and its application to the safety assessment of autonomous cars," Ph.D. dissertation, Technische Universität München, 2010.
- [8] B. Mu, X. Yang, and J. K. Scott, "Comparison of advanced set-based fault detection methods with classical data-driven and observer-based methods for uncertain nonlinear processes," *Computers & Chemical Engineering*, vol. 166, p. 107975, 2022.
- [9] T. Alamo, J. M. Bravo, and E. F. Camacho, "Guaranteed state estimation by zonotopes," *Automatica*, vol. 41, no. 6, pp. 1035–1043, 2005.
- [10] M. E. Dyer, "The complexity of vertex enumeration methods," *Mathematics of Operations Research*, vol. 8, no. 3, pp. 381–402, 1983.
- [11] C. Le Guernic and A. Girard, "Reachability analysis of hybrid systems using support functions," in *International Conference on Computer Aided Verification*, Grenoble, France, 2009, pp. 540–554.
- [12] S. Kousik, A. Dai, and G. X. Gao, "Ellipsotopes: Uniting ellipsoids and zonotopes for reachability analysis and fault detection," *IEEE Transactions on Automatic Control*, vol. 68, no. 6, pp. 3440–3452, 2022.
- [13] V. Raghuraman and J. P. Koeln, "Set operations and order reductions for constrained zonotopes," *Automatica*, vol. 139, p. 110204, 2022.
- [14] D. Silvestre, "Exact set-valued estimation using constrained convex generators for uncertain linear systems," *IFAC-PapersOnLine*, vol. 56, no. 2, pp. 9461–9466, 2023.
- [15] F. Rego and D. Silvestre, "A novel and efficient order reduction for both constrained convex generators and constrained zonotopes," *IEEE Transactions on Automatic Control*, 2025, Early Access.
- [16] J. W. Helton and J. Nie, "Sufficient and necessary conditions for semidefinite representability of convex hulls and sets," *SIAM Journal on Optimization*, vol. 20, no. 2, pp. 759–791, 2009.
- [17] J. Gouveia and T. Netzer, "Positive polynomials and projections of spectrahedra," *SIAM Journal on Optimization*, vol. 21, no. 3, pp. 960–976, 2011.
- [18] C. Scheiderer, "Spectrahedral shadows," *SIAM Journal on Applied Algebra and Geometry*, vol. 2, no. 1, pp. 26–44, 2018.
- [19] R. G. Bettiol, M. Kummer, and R. A. Mendes, "Convex algebraic geometry of curvature operators," *SIAM Journal on Applied Algebra and Geometry*, vol. 5, no. 2, pp. 200–228, 2021.
- [20] D. Silvestre, "Set-valued estimators for uncertain linear parameter-varying systems," *Systems & Control Letters*, vol. 166, p. 105311, 2022.
- [21] C. Wang, H. Liu, and F. Xu, "Performance metric and analytical gain optimality for set-based robust fault detection," *Automatica*, vol. 159, p. 111376, 2024.
- [22] M. Kvasnica, B. Takács, J. Holaza, and D. Ingole, "Reachability analysis and control synthesis for uncertain linear systems in mpt," *IFAC-PapersOnLine*, vol. 48, no. 14, pp. 302–307, 2015.
- [23] F. Borrelli, A. Bemporad, and M. Morari, *Predictive control for linear and hybrid systems*. Cambridge, UK: Cambridge University Press, 2017.
- [24] C. Combastel, "A state bounding observer based on zonotopes," in *2003 European control conference*, Cambridge, UK, 2003, pp. 2589–2594.
- [25] F. Blanchini, S. Miani et al., *Set-theoretic methods in control, 2-nd edition*. Berlin, Germany: Springer, 2015, vol. 78.
- [26] V. V. Williams, Y. Xu, Z. Xu, and R. Zhou, "New bounds for matrix multiplication: from alpha to omega," in *Proceedings of the 2024 Annual ACM-SIAM Symposium on Discrete Algorithms*, Alexandria, VA, USA, 2024, pp. 3792–3835.
- [27] N. Kochdumper and M. Althoff, "Sparse polynomial zonotopes: A novel set representation for reachability analysis," *IEEE Transactions on Automatic Control*, vol. 66, no. 9, pp. 4043–4058, 2020.
- [28] H. Jiang, T. Kathuria, Y. T. Lee, S. Padmanabhan, and Z. Song, "A faster interior point method for semidefinite programming," in *2020 IEEE 61st Annual Symposium on Foundations of Computer Science*, Durham, NC, USA, 2020, pp. 910–918.
- [29] J. W. Helton and J. Nie, "Semidefinite representation of convex sets," *Mathematical Programming*, vol. 122, pp. 21–64, 2010.
- [30] J. B. Lasserre, "Convex sets with semidefinite representation," *Mathematical Programming*, vol. 120, no. 2, pp. 457–477, 2009.
- [31] J. W. Helton and J. Nie, "Semidefinite representation of convex sets and convex hulls," *Handbook on semidefinite, conic and polynomial optimization*, pp. 77–112, 2012.
- [32] A. Nemirovski, "Advances in convex optimization: conic programming," in *International Congress of Mathematicians*, vol. 1, Madrid, Spain, 2006, pp. 413–444.
- [33] W. J. Firey, "p-means of convex bodies," *Mathematica Scandinavica*, vol. 10, pp. 17–24, 1962.
- [34] E. Lutwak, "The brunn-minkowski-firey theory. i. mixed volumes and the minkowski problem," *Journal of Differential Geometry*, vol. 38, no. 1, pp. 131–150, 1993.
- [35] R. Schneider, *Convex bodies: the Brunn-Minkowski theory*. Cambridge, UK: Cambridge university press, 2013, vol. 151.
- [36] E. Lutwak, D. Yang, and G. Zhang, "The brunn-minkowski-firey inequality for nonconvex sets," *Advances in Applied Mathematics*, vol. 48, no. 2, pp. 407–413, 2012.
- [37] A. Ben-Tal and A. Nemirovski, *Lectures on Modern Convex Optimization: Analysis, Algorithms, and Engineering Applications*. Philadelphia, PA, USA: SIAM, 2001.
- [38] F. Xu, "Minimal detectable and isolable faults of active fault diagnosis," *IEEE Transactions on Automatic Control*, vol. 68, no. 2, pp. 1138–1145, 2022.
- [39] R. A. Horn and C. R. Johnson, *Matrix Analysis*. Cambridge, UK: Cambridge university press, 1985.
- [40] A. M. Sletsjøe, "Spectrahedra and their boundaries," Master's thesis, Department of Mathematics, University of Oslo, 2023.
- [41] K. Kellner, T. Theobald, and C. Trabant, "Containment problems for polytopes and spectrahedra," *SIAM Journal on Optimization*, vol. 23, no. 2, pp. 1000–1020, 2013.
- [42] L. Lovisolo and E. Da Silva, "Uniform distribution of points on a hypersphere with applications to vector bit-plane encoding," *IEEE Proceedings-Vision, Image and Signal Processing*, vol. 148, no. 3, pp. 187–193, 2001.
- [43] M. ApS, *The MOSEK optimization toolbox for MATLAB manual. Version 10.2.*, 2024. [Online]. Available: <http://docs.mosek.com/latest/toolbox/index.html>
- [44] M. Ramana and A. J. Goldman, "Some geometric results in semidefinite programming," *Journal of Global Optimization*, vol. 7, no. 1, pp. 33–50, 1995.
- [45] S. Boyd and L. Vandenberghe, *Convex Optimization*. Cambridge, U.K.: Cambridge university press, 2004.
- [46] J. W. Helton, I. Klep, and S. McCullough, "The matricial relaxation of a linear matrix inequality," *Mathematical Programming*, vol. 138, no. 1, pp. 401–445, 2013.